MASS SPECTROMETRY IN NUCLEAR CHEMISTRY

H. G. Thode, C. C. McMullen, and K. Fritze

Departments of Chemistry and Physics, McMaster University, Hamilton, Ontario, Canada

I. Introduction

Mass spectrometers have been used extensively in the field of nuclear chemistry, and the development of instruments of high sensitivity in recent years has made them indispensable tools in this field. In particular, the use of isotope dilution techniques has extended the usefulness of mass spectrometers in the solution of nuclear problems.

The important developments in nuclear chemistry in which mass spectrometers have played a role will be reviewed in this chapter. These include the identification and determination of radioactive isotopes and of stable daughter products in nature, the accurate determination of half-lives for

certain radioactive isotopes, neutron cross sections of both stable and radioactive isotopes, and, finally, the accurate determination of mass chain yields and independent yields of fission products from the various elements which undergo fission.

In all these applications, sensitive instruments for the determination of isotope abundances are required. In this connection, the conventional ionic-type mass spectrometer is used almost exclusively for the determination of absolute and relative isotope abundances with the exception of the wide use of infrared methods for the determination of hydrogen to deuterium ratios.

The early mass spectrographs or mass spectrometers, were used mainly to identify the isotopes of the elements and to measure their abundances. Using the parabola method of positive ion analysis, J. J. Thomson (*107*) showed conclusively that the element neon consisted of at least two types of atoms, one of mass 20 and the other of mass 22. A third stable isotope of mass 21 was later shown to exist. In 1919, Aston (*6*) designed the first "mass spectrograph" which could be used to measure isotope abundances and succeeded in making abundance determinations of a number of elements. In 1918, Dempster (*24*) developed a new type of instrument which employed a method used earlier by Classen (*20*) to determine the electron charge-to-mass ratio. This instrument which uses the geometric focusing properties of a homogeneous magnetic field on a stream of charged particles, forms the basis of most ionic-type mass spectroscopes used today. These instruments are comprised of four basic components, a sample system, an ion source, an analyzer, and an ion-detector system. In general, ions which are produced at the source, either by electron impact or by thermionic emission from a hot filament, are accelerated by a voltage V through a system of slits. The beam of ions produced is then deflected by a uniform magnetic field H in the analyzer, according to the relation:

$$e/m \propto 2V/H^2R^2, \tag{1}$$

where e is the ionic charge, m is the mass, and R the radius of curvature of the ion path in the magnetic field. By a suitable adjustment of the parameters V and H, ions of any desired mass may be collected by a Faraday cup and measured. The measured current of positive ions is the basis of relative abundance calculations.

By 1930, Aston and Dempster, between them, had investigated the isotopes of most of the then known elements. However, their instruments were of low sensitivity and many isotopes were missed. For example, Aston in his work on the isotopes of ruthenium (*7*) was unable to detect Ru^{98} which was later found to have a natural abundance of 1.9%. Also, the iso-

topes C^{13}, N^{15}, O^{17}, and O^{18} went undiscovered until the late 20's when their existence was established by optical spectroscopy (*45*).

A. Instrumental Sensitivity

Following the pioneer work of Aston and Dempster, there were rather limited advances made in the field of isotopic abundance measurements until 1935 when A. O. Nier (*85*) introduced a number of improvements to mass spectrometer design. Since then, many more refinements have been made, particularly with regard to more efficient ion sources and to more sensitive ion detectors, so much so, that the mass spectrometer has become an extremely sensitive instrument for the detection of practically all of the elements, and its sensitivity remains second only to that of radioactive counting techniques.

With the development of the electron multiplier by Bay (*10*) and Allen (*3*) and its subsequent incorporation into a mass spectrometer as an ion detector (*21*), it has been possible to increase the sensitivity of a standard mass spectrometer by as much as a factor of 10^4.

Also new and more efficient ion sources have been produced both for gas and solid samples (*8*). For example, Inghram (*56*) modified a surface ionization source to incorporate three filaments and succeeded in analyzing samples of the heavy elements as small as 10^{-12} gm, when the source is used in conjunction with an electron multiplier detector. The over-all efficiency of a surface ionization source depends upon the number of neutral molecules impinging on the ionization surface at the operating temperature of the filament. In the case of many elements which have high ionization potentials, it is found that the vapor pressure of the compound containing the element reaches a high value before a suitable ionization temperature can be achieved. The multiple filament source circumvents this difficulty when the sample is dried on one of two sample filaments which are in close proximity to a high temperature ionizing filament. By controlling the current in the sample filament, it is possible to set the sample evaporation rate at any given level. The neutral atoms which then impinge on the hot ionization filament are ionized and accelerated into the magnetic analyzer.

F. A. White *et al.* (*120*) have employed a filament which is folded in the shape of a V into which the sample is placed. Neutral atoms which are evaporated from the hot tungsten are given an additional opportunity to become ionized on the walls of the tungsten V before they reach the first slit of the ion source. Both the V-shaped filament and the multifilament ion sources have proved successful in improving the efficiency of ion production for elements having high ionization potentials.

B. Absolute Abundance Measurements

Sources of error in isotope abundance measurements have been discussed in detail elsewhere (*106*). The reproducibility of results with a modern instrument is usually better than 0.1%. Furthermore, it is possible to detect differences in isotope ratios of better than 0.02% using isotope ratio instruments which employ simultaneous ion collection systems. These high-precision isotope ratio instruments are used extensively to study equilibrium and kinetic isotope effects in chemistry and to measure the variations in isotope abundances that occur in nature.

Although the isotope ratios of samples may be compared with high precision, the absolute errors may be quite large, usually of the order of 1.0%. These errors may be attributed to the method of introducing the sample into the mass spectrometer or to discriminating effects within the ion source, analyzer, or detector regions of the instrument (*26*).

For the mass spectrometric analysis of gaseous elements, the sample is introduced into the ionization chamber through what is known as a "leak." Molecular flow will occur through the leak when the mean free path of the molecules is at least 10 times greater than the diameter of the leak. The velocity of flow will then be inversely proportional to the square root of the isotopic mass. At the same time, molecular flow will occur when the gases are pumped out of the ionization chamber. Provided the volume of the gas reservoir behind the leak is large so that depletion of a light isotope is small during analysis, cancellation of the discrimination in the gas flow system occurs. Thus the gas in the ionization chamber will have the same composition as that of the reservoir.

On the other hand, viscous flow will dominate in the leak when conditions are such that the mean free path is small compared to the leak dimensions. In this instance, the flow rate is independent of the isotopic mass and a correction which is proportional to $1/\sqrt{M}$ is necessary to compensate for molecular flow from the ionization chamber.

When analyzing elements which are ionized by evaporation from an oven or heated surface, isotopic fractionation is once again a serious problem. This fractionation which again depends upon $1/\sqrt{M}$ is large when the isotopic masses are small. It is therefore essential that each ionization process be investigated to determine the amount of discrimination which occurs during the analysis of a particular element.

When electron impact sources are employed, some mass discrimination effects can be attributed to space charges which build up in the ionization chamber. The magnitude of these effects may be determined by measuring the isotope ratio as a function of the ionizing current and then extrapolating to zero current. In addition, isotope effects may occur in the dissociation

of molecules by electron impact. Since there is no satisfactory explanation for this phenomenon, care must be exercised when mass spectrometric studies of molecular species are undertaken (*106*).

Other effects which are of a minor nature but still require attention when making absolute abundance measurements are those which occur in the analyzer tube and at the collector. Residual gases in the instrument can provide a source of error when weak ion currents are being measured. These can usually be minimized by baking the spectrometer at temperatures between 300° and 400°C in order to outgas the entire source and analyzer system before the sample is introduced. Small angle ion scattering can, in general, be overcome to a large extent by proper design of the instrument. The tandem analyzer design of Inghram and Hess (*58*) and White and Collins (*118*) practically eliminates this effect and it is then possible to measure the ion currents of adjacent masses which have an abundance ratio of approximately 10^8. This type of "tandem" or double analyzer mass spectrometer is being used in a number of laboratories to determine either a rare isotope in nature (*119*, *120*) or the formation of an isotope in some nuclear process, in each case in the presence of a very high concentration of the adjacent or target isotope. Such instruments are, of course, ideal for the study of certain $(n, 2n)$ reactions and are perhaps the ultimate in low-level detection work. It should be pointed out, however, that the abundance sensitivity of mass spectrometers using a single magnetic analyzer may be considerably improved by using improved pumping systems and operating at lower pressures.

At the collector, secondary electron emission, which occurs when the energetic ions are stopped, is prevented by incorporation of a suppressor grid in the detector assembly. A less elegant method is to collect the ions in a long V-shaped electrode from which very few secondary electrons will escape. When an electron multiplier is employed to detect the ions, a mass discrimination will occur when the integrated electron current from the multiplier is used as a measure of the ion current. When pulse-counting techniques are used to detect the ions, this discrimination disappears provided each ion produces an electron pulse which is of sufficient magnitude to be counted by some counting rate-measuring device. It is obvious that accurate absolute abundance measurements require very careful studies of a number of discrimination effects which occur in the mass spectrometer if an absolute accuracy of the order of 0.1% is to be achieved.

In 1950, Nier (*86*) reported the redetermination of the relative abundances of the isotopes of a number of elements with an accuracy of 0.1%. The mass spectrometer used in these studies was calibrated for mass discrimination effects by means of carefully prepared synthetic mixtures of A^{36} and A^{40}. Samples of elements for which accurate isotope ratios are

known may be used as secondary standards for instrument calibration purposes.

C. Contamination Problems

Ever since the time of Aston, contamination problems have plagued the mass spectroscopists. Ions of hydrocarbon fragments which fall at almost every mass present a serious problem. These contamination problems are even greater when instruments of high sensitivity are used in low-level detection work. Small residual ion currents due to hydrocarbons persist even after long baking and inert gas flushing of the mass spectrom-

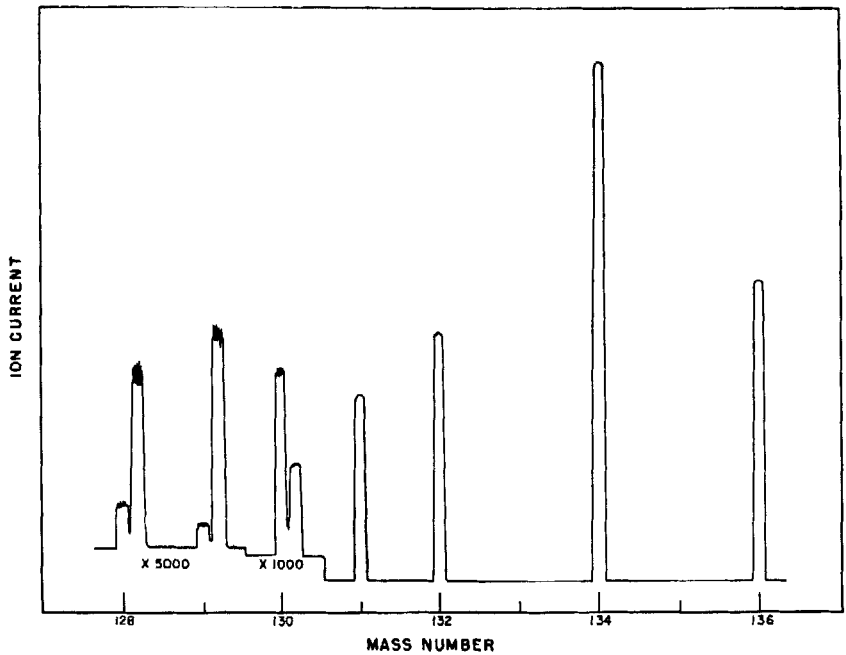

Fig 1. Mass spectrogram of the xenon isotopes for the thermal neutron fission of Pu^{239} (*62*).

eter. However, the hydrocarbon problem may be overcome by increasing the resolution of the instrument until the isotopic masses in question are resolved from the hydrocarbons corresponding to the same masses. This may be done with conventional instruments simply by using narrower entrance and exit slits in the mass spectrometer, providing the instrument sensitivity is sufficient to measure the decreased ion currents which result. Figure 1 shows a mass spectrogram of the xenon isotopes in a sample of

fission gas from the neutron-induced fission of Pu^{239} (*62*). The isotopes Xe^{131}, Xe^{132}, Xe^{134}, and Xe^{136} are all produced in high yield and hydrocarbon contamination "peaks" did not show up at the low sensitivities used to measure them. However, in the case of the isotopes of Xe^{128}, Xe^{129}, and Xe^{130}, measured at sensitivities 1000 to 5000 times higher, small hydrocarbon peaks did appear on the high mass side of each isotopic peak. When these doublets are completely resolved it is then possible to identify and measure rare isotopes such as Xe^{128} even though the hydrocarbon contamination produces 4 times the ion current. In the particular example shown in Fig. 1, the sample contained approximately 10^{-12} gm of Xe^{128}. The limit of detection in this case was of the order of 10^{-13} gm.

D. Isotope Dilution

The mass spectrometer method of chemical analysis which employs isotope dilution techniques has wide application in nuclear chemistry and physics, particularly in low-level detection work. There are many problems which require a quantitative measure of the amount of a particular element or isotope present in a sample in amounts less than one part per million. Sensitive mass spectrometers and the availability of tracer isotopes make the solution of these problems possible.

The isotope dilution method first proposed by Hevesy (*49*) has been used extensively by Rittenberg (*94*) with stable isotope tracers for the determination of the elements and compounds of hydrogen, carbon, and nitrogen. Now that separated isotopes of many elements are more readily available, the method has been greatly extended and the isotope dilution technique has become a very effective tool in quantitative trace analysis. By adding to a sample a known amount of a separated or enriched isotope of the element under study and then measuring by means of a mass spectrometer, the resulting change in the isotopic abundances of the element, it is possible to calculate the absolute number of atoms which were present in the original samples. For example, Xe^{128} which is produced by neutron irradiation of I^{127} ($I^{127} \xrightarrow{n} I^{128} \xrightarrow{\beta^-} Xe^{128}$) may be used as a tracer isotope in the absolute determination of xenon. In this case, a small quantity of Xe^{128} tracer is measured out with a system of gas pipettes and added to the gaseous sample. The xenon may then be extracted from the sample employing the usual techniques of rare gas purification. Finally, the change in isotopic composition of the xenon is determined mass spectrometrically. From this procedure, the number of atoms of the various isotopes of xenon in the original sample may be determined. In cases where it is known that the isotopic composition of the element under investigation is different from the com-

position found in nature (for example, fission products), measured quantities of the normal element can be used as diluent. In the isotope dilution method, the tracer is measured and added to the sample under study prior to any chemical separation of the element in question. A quantitative recovery of the tracer and unknown is then unnecessary since the analysis depends only on the ratio of the isotopes in the tracer-unknown mixture which is not significantly affected by separation procedures. This is an important feature of the method since it is very difficult and tedious to obtain 100% yields in trace analysis. A hypothetical isotope dilution measurement of lanthanum in a solid sample (*59*) is illustrated in Fig. 2.

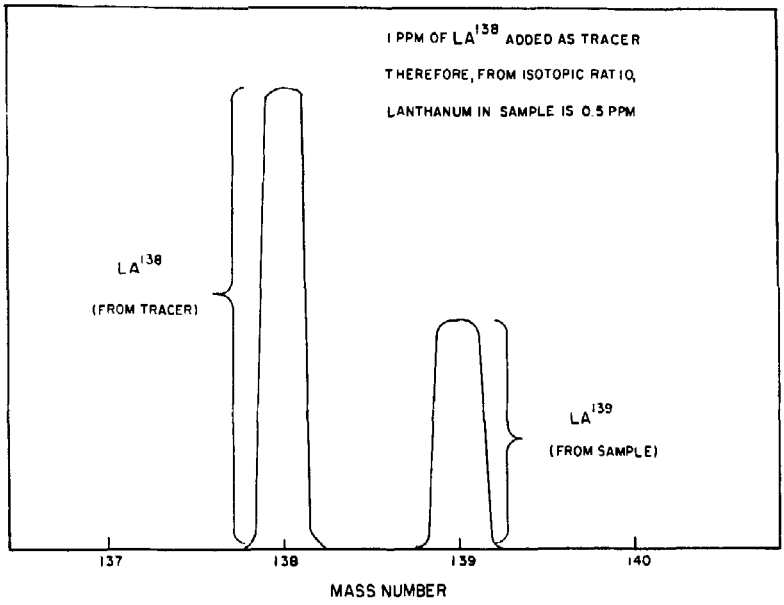

FIG. 2. Hypothetical isotope dilution determination of lanthanum (*59*).

One serious difficulty which is encountered in the determination of minute samples or of trace impurities in a sample is that of contamination from reagents. By analyzing samples of different size it is possible to evaluate the extent of this interference. In general, extreme care must be taken in the preparation of reagents to ensure that the contamination by trace quantities of an element is reduced to a level which can be tolerated.

Since stable isotope dilution depends on the mass spectrometric determination of isotope ratios, the method is generally restricted to elements which have at least two stable isotopes. However, in the case of mono isotopic cesium, the long-lived fission product Cs^{135} or Cs^{137} can be used as a tracer for the analysis of this element. In all, some 68 elements can be

analyzed by this method (*57*). Modern mass spectrometers which employ electron multipliers for ion detection may detect as little as 10^{-12} gm of most elements. In the case of gas analysis it has been possible, using high-vacuum techniques, to measure 1 part in 10^8 of krypton in xenon (*117*). By eliminating the difficulty with gas scattering it should be possible to obtain sensitivities of 1 part in 10^{10}.

Application of trace element techniques has brought fruitful results in the area of nuclear science. Some of the important results obtained to date are discussed in the following sections.

II. Mass Assignment

During the last 25 years, a large number of radioactive species has been discovered. One of the prime objectives of nuclear chemists has been to assign the atomic number and the mass number to the nuclides which are responsible for observed activities. In general, the atomic number is found by chemical analysis, whereas the mass assignment is most unambiguously obtained by methods involving mass spectrometric techniques.

As early as 1937, Smythe and Hemmendinger (*97*) separated the isotopes of potassium in a high intensity mass spectrometer and showed conclusively that the activity which had been discovered 30 years earlier (*19*) is associated with K^{40}. In the same year, the known β-activity of natural rubidium was assigned to Rb^{87} using two different methods. Hemmendinger and Smythe (*46*) used exactly the same experiment as for potassium, whereas Mattauch (*78*) showed that strontium isolated from an old rubidium-rich mineral was essentially pure Sr^{87} (see also Section III). Since 1945, mass assignments have been made to nearly 200 artificially produced radioactive species. This has been made possible on the one hand by the enormous development in instrumentation during the war years and, on the other hand, by the ability to produce a large number of radioactive isotopes in sufficient quantity to allow this type of study. One technique uses a mass spectrograph to separate the isotopes which are deposited either on photographic plates or on metal collectors. In the photographic method, the known spectrum of the stable element is used for mass calibration. Any additional lines can be attributed to artificially produced isotopes and activities can be assigned to their respective masses using the "transfer plate" technique (*43*).

In this method a second photographic plate is placed in contact with the original collector plate. The radiations emitted by any radioactive nuclide cause, after a suitable exposure, a blackening on the second plate and thus makes possible the identification of the nuclide or nuclides responsible for the radioactivity. An alternative method is to scan the first plate with a

radiation detector having a fine slit. These techniques have been widely used by workers in this field (*41*, *71*, *72*, *93*).

Approximate measurements of the half-life have been employed, whenever possible, to establish the identity of the radioactive species involved. If a line corresponding to one isotope is found on the transfer plate, mass assignment of the activity is certain. However, if the transfer plate shows more than one line, a rough half-life measurement must be made in order to associate the proper mass with the accurate half-life obtained from other experiments. For example, Hess *et al.* (*47*) analyzed neutron-irradiated rhenium in a mass spectrograph, collecting the ions on a photographic plate. Two successive radioautographs of this plate were made, the first one being exposed for 36 hr, the second one for 180 hr. All three plates were then developed and comparisons of the lines made, using the primary plate as a mass marker. The 36-hour plate showed two weak lines at masses 186 and 188, whereas, the second plate revealed only one line at mass 186. On the other hand, the decay curve for neutron-irradiated rhenium can be resolved into two components having half-lives of 17 hr (*73*) and 91 hr (*22*). Since no line appeared at mass 188 on the second transfer plate the shorter of the two half-lives must be associated with this rhenium isotope.

Instead of the conventional mass spectrograph, other types of mass spectroscopes have been used in an effort to obtain mass assignments. A time-of-flight mass separator, constructed at the University of California, has been used extensively to study high-energy fission and spallation products (*83*). This instrument features an absolute mass calibration which renders unnecessary the observation of ion currents from isotopes of known mass. The investigation of iodine isotopes obtained as spallation products of cesium (*1*) is an example of the use of electromagnetic isotope separators not only for mass assignment purposes but also for obtaining correct values for the half-lives of several isotopes of the same element. Normally, the isotopes are collected on thin metal foils which are cut into strips for counting, each strip containing the atoms which have been collected at one mass position.

III. Half-life Determinations

The obvious method of determining the half-life of a radioactive sample is to measure the change in activity of the sample in successive intervals of time. Another satisfactory procedure is to measure the disappearance of a radioactive parent nuclide or the growth of a daughter nuclide using mass spectrometric techniques. In the former method, emitted particles are counted, whereas, the latter method measures directly the decrease in the amount of the parent isotope, or the increase in the amount of the

daughter isotope, both relative to a stable isotope of their respective element. In addition, a combination of counting and mass spectrometric measurements can be used effectively to measure half-lives which cannot be readily determined by other methods.

A. Decay Method

The half-life $T_{\frac{1}{2}}$ of any radioactive species is given by the following equation:

$$T_{\frac{1}{2}} = -0.693t/(\ln N/N_0), \tag{2}$$

where N/N_0 is the fraction of the atoms remaining after a decay time t. Thode and his collaborators (*104*, *112*) who discovered the long-lived fission product Kr^{85}, have assigned its half-life as 10.27 ± 0.18 yr by measuring several times during a period of 7 yr the change in Kr^{85}/Kr^{84} and Kr^{85}/Kr^{86} ratio. Since both Kr^{84} and Kr^{86} are stable isotopes, the measured ratios can be used directly to obtain N/N_0. In principle, either of the two ratios is sufficient to determine $T_{\frac{1}{2}}$. However, the Kr^{86}/Kr^{84} ratio provides a means of correcting for any normal krypton which could be introduced accidentally because of frequent handling of the sample over a long period of time. Essentially the same procedure has been used to determine the 5.271 ± 0.002-day half-life of Xe^{133} (*74*) and a 33 ± 2-yr half-life of Cs^{137} (*121*). Half-lives, ranging from about 50 yr to a few days, can be determined using this method. The lower half-life limit is governed by the difficulty in obtaining a sufficient quantity of the isotope in question for mass spectrometric analysis. Since the sensitivity of mass spectrometers changes from element to element, this lower limit cannot be well defined. As in the case of counting techniques, the upper half-life limit is determined by the length of time during which observations are made relative to the half-life of the isotope under study.

B. Daughter-Growth Method

Since each radioactive decay forms one atom of a different element, the accumulation of the daughter product can be followed as a function of time. This build-up can be expressed by the following equation:

$$N_d = N_0\left[1 - \left(\exp - \frac{0.693t}{T_{\frac{1}{2}}}\right)\right], \tag{3}$$

where N_d is the number of daughter atoms; N_0 the number of parent atoms at $t = 0$; t the elapsed time; and $T_{\frac{1}{2}}$, the half-life of the parent isotope. Since the fractional change in N_d is particularly large for values of t which

are small in comparison to the half-life, the daughter-growth method permits a more accurate determination of long half-lives in a relatively short period of time. For example, work is in progress in this laboratory to determine, mass spectrometrically, the amount of Sr^{87} which has been formed from the β-decay of the Rb^{87} in 20-gm samples of strontium-free rubidium perchlorate. Using the currently accepted half-life of 5×10^{10} yr (*2*) for Rb^{87} approximately 7×10^{-11} gm of Sr^{87} would be formed during a 2-yr period. It is felt that this quantity of Sr^{87} can be accurately determined employing a known amount of Sr^{90} for isotope dilution. In principle, the same approach was used in 1938 when Strassmann and Walling (*101*) analyzed an old mica from Manitoba, Canada, for its rubidium and strontium content. They calculated the half-life (6.3×10^{10} yr) from the geological age of the mineral after Mattauch (*78*) had proven, mass spectrographically, that the chemically isolated strontium consisted of 99.7% Sr^{87}. By a careful analysis of several minerals from a number of pegmatites, using isotope dilution methods, Aldrich and his co-workers (*2*) have shown the half-life of Rb^{87} to be $(5.0 \pm 0.2) \times 10^{10}$ yr. However, in experiments of this kind, the accuracy of the half-life is limited by the value obtained for the geological age, a difficulty which is circumvented in the experiment discussed above.

C. Specific Activity Method

Another accurate, but experimentally more difficult, method of determining the half-life is to evaluate the components of the differential decay equation:

$$T_{\frac{1}{2}} = -\frac{0.693}{dN/dt} \times N. \tag{4}$$

The disintegration rate, dN/dt can be measured by absolute counting and the number of atoms N determined by means of mass spectrometric techniques. Bartholomew *et al.* (*9*) isolated the chlorine from irradiated KCl and measured the disintegration rate of a known amount of chlorine using 4π beta counting methods. Another portion was analyzed by means of a mass spectrometer for the Cl^{36} content. Combining these results, they obtained a half-life of 3.08×10^{6} yr for Cl^{36}. In cases where the amount of the radioactive isotope is small, aliquots of a stock solution of the element are used for 4π counting and to determine the concentration by means of isotope dilution. This procedure was followed by Wiles and Tomlinson (*122*) and by Brown *et al.* (*16*) to determine the half-life for Cs^{137}. The difference in the results of the two groups (26.6 yr and 30.0 yr, respectively) is difficult to explain since the corrections applied to the 4π counting meas-

urements were essentially the same in both cases. This method has been used to determine the half-life of Be^{10} (*80*), Sr^{90} (*123*), U^{232} (*96*), and other isotopes.

IV. Neutron Capture Cross Sections

Although a number of different reactions can be initiated when an element is irradiated with neutrons, this discussion will be restricted essentially to slow neutron reactions of the (n,γ) type. These reactions produce a mass increase of unity in any isotope involved and, consequently, cause a change in the isotopic composition. The magnitude of these changes will be determined for the various isotopes by the neutron capture cross section, the neutron flux, and the irradiation time.

Quantitatively the (n,γ) reaction can be described by the following equation:

$$N = N_0 e^{-\sigma_c \phi t}, \tag{5}$$

where N_0 is the number of target nuclei at the beginning of the irradiation; N, the number of target nuclei remaining at the end of the irradiation; σ_c, the capture cross section; ϕ, the neutron flux; and t, the irradiation time.

The form of this equation immediately suggests that the approach to measure cross sections is similar to the one used for the determination of half-lives. However, cross section measurements are complicated by the fact that σ_c is a function of the neutron energy and by the difficulty in obtaining a reliable value of the neutron flux. The product isotope of an (n, γ) reaction can be either radioactive or stable. In the former case, either counting methods or mass spectrometric techniques can be utilized in order to obtain information concerning the capture cross section. When the product isotope is stable, only mass spectrometric methods are applicable.

A. Quantitative Determinations

Dempster (*25*) for the first time showed that the isotopic composition of an element could be modified by a long neutron irradiation and proved conclusively that Cd^{113} was responsible for the large cross section which had been observed previously in normal cadmium. His spectrograms of irradiated cadmium revealed a marked decrease in the intensity of the Cd^{113} line and a corresponding enhancement of the Cd^{114} line. Lapp, Van Horn, and Dempster (*68*) also showed that the large cross section found in samarium and gadolinium could be attributed to the isotopes Sm^{149}, Gd^{155}, and Gd^{157}. Figure 3 shows a mass spectrogram of the gadolinium isotopes before and after irradiation with thermal neutrons. It can be seen that

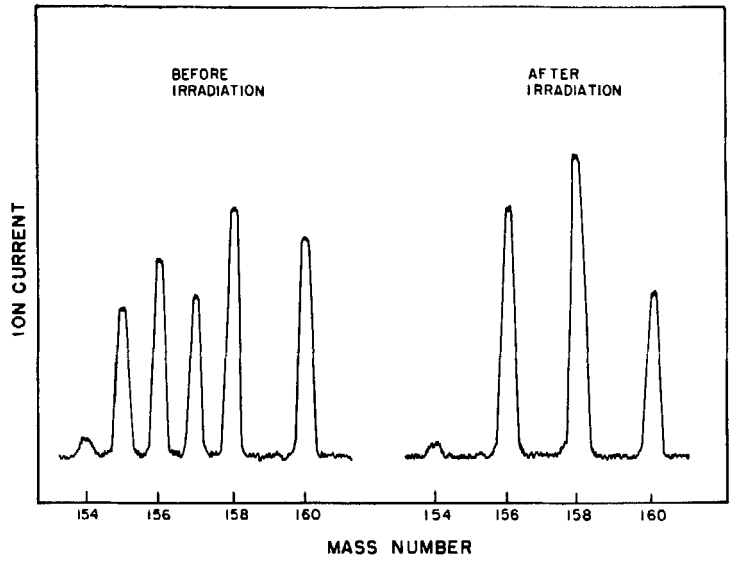

FIG. 3. Mass spectrogram of gadolinium before and after thermal neutron irradiation (*110*).

Gd^{155} and Gd^{157} have been completely converted to Gd^{156} and Gd^{158}, respectively, as a result of neutron absorption.

B. Relative Cross Sections

With a mass spectrometer it is possible to measure relative changes in isotopic composition very accurately. One can, therefore, obtain some quantitative information concerning capture cross sections. In the case of a hypothetical element consisting of three stable isotopes, A, B, and C, having successive masses where A and C have measurable cross sections, the number of atoms of the different isotopes, after an irradiation of time duration t, can be expressed as follows:

$$N_{At} = N_{A0}\, e^{-\sigma_A \phi t}, \tag{6}$$

$$N_{Bt} = N_{B0} + N_{A0}(1 - e^{-\sigma_A \phi t}), \tag{7}$$

$$N_{Ct} = N_{C0}\, e^{-\sigma_C \phi t}, \tag{8}$$

where N_{At}, N_{Bt}, N_{Ct} are the number of atoms of isotopes A, B, and C after the irradiation; N_{A0}, N_{B0}, N_{C0} are the number of atoms of isotopes A, B, and C at the beginning of the irradiation ($t = 0$); σ_A, σ_C, the neutron capture cross section of isotopes A and C, respectively; ϕ, the neutron flux; and t, the irradiation time.

By combining Eqs. (6), (7), and (8), the following expression relating σ_A and σ_C can be derived:

$$\frac{\sigma_C}{\sigma_A} = \frac{\ln (N_{Ct}/N_{At}) + \ln (N_{A0}/N_{C0})}{\ln (N_{Bt}/N_{At} + 1) - \ln (N_{B0}/N_{A0} + 1)}. \tag{9}$$

The values for N_{A0}/N_{C0} and N_{B0}/N_{A0} are obtained from the known abundances of the element before irradiation, whereas, N_{Ct}/N_{At} and N_{Bt}/N_{At} can be calculated from the results of the mass spectrometric analysis of the irradiated material. The accuracy of spectrometric measurements are usually good to $\pm 0.5\%$ or better.

It should be realized that this hypothetical example is a rather simple one and in practice, the problem is frequently complicated by one or more of the following factors: (1) the number of stable isotopes is larger; (2) some of the irradiation products are radioactive but have a considerable cross section which might lead to another stable isotope; (3) the capture of a neutron by a particular isotope can produce isomers, which, in turn, are likely to have different cross sections (in this case also the branching ratio for the production of the two isomers would have to be taken into account); (4) if the irradiation position in the reactor is such that the contribution of fast neutrons is significant, allowance may have to be made for other types of nuclear reactions. It is obvious that these complicating factors will make the mathematical treatment more complex. In this connection, the reader is referred to a paper by Hayden, Reynolds, and Inghram (*44*) which deals with the reactions induced in europium by slow neutrons. Studies of the isotopic capture cross sections of a number of other elements have been performed by other workers (*48*, *54*, *111*).

C. Absolute Cross Sections

It will be noted in most of the publications that absolute capture cross sections have been tabulated. In order to convert from relative to absolute isotopic cross sections, a knowledge of the absolute elemental cross section is required. Since the elemental cross sections are rarely known to better than $\pm 10\%$, the error in the isotopic cross section will be determined by the accuracy of the assigned elemental cross sections.

If Eq. (5) is rewritten in the following form

$$\sigma = (\ln N/N_0)/\phi t, \tag{10}$$

it can be seen that a mass spectrometric determination of N/N_0 and a knowledge of the integrated neutron flux ϕt, will permit an evaluation of the absolute capture cross section. The integrated flux can be determined by the simultaneous irradiation of a flux monitor with the sample. Boron

and cobalt have been used for this purpose (*35, 91*). In the former case, the change in the B^{10}/B^{11} ratio resulting from the B^{10} (n,α) Li^7 reaction is measured and ϕt calculated, using the known B^{10} cross section

$$\phi t = \ln \frac{B_0^{10}}{B_t^{10}} \times \frac{1}{\sigma_{B^{10}}}.$$

In the latter case, the disintegration rate of Co^{60} produced during the irradiation is measured and ϕt calculated using this information

$$\phi t = \frac{dN_{60}}{dt} \times \frac{1}{\lambda_{60}} \times \frac{1}{N_{59}} \times \frac{1}{\sigma_{59}}.$$

The accuracy of the value of the integrated flux will be largely determined by the accuracy of the cross section assigned to the monitor material.

Up to this point, discussion has been restricted to multi-isotope elements. Since one obtains only isotopic ratios from mass spectrometric analyses, the disappearance of a single isotope cannot be measured directly if the radioactive product is short-lived. However, in principle, a method which is very similar to the daughter-growth method for determining half-lives (Section III) should be applicable. For example, the neutron irradiation of Au^{197} yields Au^{198} which decays with a 2.70-day half-life to Hg^{198}. After a suitable irradiation and decay time, the gold is dissolved, a known quantity of mercury added, and the isolated mercury analyzed in a mass spectrometer. From the increase in the Hg^{198}/Hg^{199} ratio the number of Au^{198} atoms produced can be calculated. As a result, the cross section can be obtained providing the neutron flux ϕ is sufficiently small that the Au^{198} (n,γ) Au^{199} reaction is of no consequence.

The largest neutron capture cross section ever found is the one for Xe^{135}. This isotope which has a 9.2-hr half-life (*61*) is one of the high yield fission products and, therefore, an exact knowledge of its cross section is extremely important from the standpoint of nuclear technology. The fission product chains involving Xe^{135} and Xe^{136} can be represented as follows (*61*):

$$\begin{array}{l} \qquad\qquad\qquad\quad \nearrow 15.3m\ Xe^{135m} \\ Te^{135} \rightarrow 6.7h\ I^{135} \qquad\quad \downarrow \qquad\quad 3 \times 10^6 y\ Cs^{135} \rightarrow \text{stable } Ba^{135} \\ \qquad\qquad\qquad\quad \searrow 9.2h\ \ Xe^{135} \nearrow \\ \qquad\qquad\qquad\quad\ \ \downarrow + n \\ Te^{136} \rightarrow 86s\ \ I^{136} \rightarrow \text{stable } Xe^{136} \end{array} \qquad (11)$$

If the irradiation of the fissile material is carried out at a low neutron flux the Xe^{135} (n,γ) Xe^{136} reaction will not significantly alter the cumulative yields of the Xe^{135} and Xe^{136} mass chains. As the flux increases, the number of Xe^{135} atoms present at any time will become larger and a significant increase in the yield of the 136 mass chain, at the expense of the 135 mass

chain, will result. Equation (12) gives the fractional increase of Xe^{136} owing to neutron capture of Xe^{135} during an irradiation.

$$\frac{\overset{\nearrow}{Xe}{}^{136}\uparrow Xe^{135}}{\underset{\nearrow}{Xe}{}^{136}\uparrow I^{136}} = \frac{\int_{t=0}^{t=T} (\text{No. atoms } Xe^{135} \text{ present at any time } t) \times F \times \sigma_{Xe^{135}}\, dt}{Y_{I^{136}} \times fT} \tag{12}$$

where F is the thermal neutron flux (neutrons $cm^{-2}\ hr^{-1}$); $\sigma_{Xe^{135}}$, the thermal neutron capture cross section for Xe^{135}; $Y_{I^{136}}$, the fission yield of I^{136}; f, the total number of fissions per hour; and T, the irradiation time (hr).

This increase can be determined by measuring either the cesium or xenon isotopic ratios. These results combined with the low flux fission yields can then be used to calculate the cross section of Xe^{135}. The ideal experiment would be one in which the flux remains constant during the entire irradiation so that the amount of Xe^{135} present at any time is not dependent on flux variations. This approach has been used by Fickel and Tomlinson (*28*), who arrived at a value of 3.2×10^6 barns (1 barn = 10^{-24} cm^2) for the neutron cross section of Xe^{135}. Cross sections of other fission products have been measured (*12*, *63*, *76*) although the conditions in these experiments were such that the effect of flux variations could not be evaluated.

D. Effective Cross Sections

In order to produce changes in isotopic composition of sufficient magnitude to be measured by a mass spectrometer, it is necessary to utilize the high neutron flux obtainable in a nuclear reactor. This flux will consist of neutrons having widely varying energy; and in the case of a well-moderated reactor, the neutron spectrum can be thought to consist of a Maxwellian distribution in energy with an added epithermal component which varies inversely as the neutron energy. The neutron temperature which corresponds to the classical temperature of the Maxwellian component can be expected to vary from one point to another in the reactor. In other words, the neutron energy spectrum will depend on the reactor geometry. It is obvious that any value for the capture cross section computed from mass spectrometric data will only represent that so-called effective cross section for the particular irradiation position. This effect will be most pronounced in cases where the cross section departs markedly from a $1/v$ energy dependence (neutron resonances). Although such cross-section results are of considerable value to reactor technologists, it would be more satisfactory to express these cross sections as the value for 2200-meters/sec neutrons. Westcott (*115*) describes the effective cross section by the following equation:

$$\hat{\sigma} = \sigma_0(g + rs), \tag{13}$$

where σ_0 is the 2200-meters/sec cross section, g and s are a measure of the departure of the cross section from a $1/v$ form (for a $1/v$ law: $g = 1$ and $s = 0$), and r measures the relative number of epithermal neutrons in the neutron spectrum. For further details concerning the effective cross section for a number of isotopes the reader is referred to the publication of Westcott (*116*).

V. Fission Yields

A. Introduction

Since the discovery of fission, a great effort has been made to unravel the maze of fission products which are produced in the various fission processes. In this work, mass spectrometric methods have been used extensively. These methods have been particularly fruitful in the determination of relative and absolute fission yields.

In the fission of a heavy nucleus, many products are formed in detectable amounts throughout the mass region 72 to 161. In general, thermal neutron fission results in two unequal mass fragments which fly apart with a total kinetic energy of about 170 Mev. The most probable heavy mass is around 139 and the most probable light mass is around 95.

Since the primary fragments formed have excitation energies of about 11 and 9 Mev for the light and heavy fragments, respectively, they disintegrate by neutron emission (*114*). It is evident from the asymmetry of fission neutron emission (*125*) that these neutrons, referred to as prompt neutrons, are emitted after the fragments have acquired 90% of their kinetic energy, the decay constant of the highly excited fragments being less than 2×10^{13} sec^{-1}. The average number of neutrons emitted per fission ν is 2.47, 2.51, 2.90 for the thermal neutron induced fission of U^{235}, U^{233}, and Pu^{239} (*114*).

The mechanisms and data of the fission process have been reviewed recently by Leachman (*70*). Several different approaches have been used in an effort to explain the asymmetry of the fission process as well as other fission parameters. These approaches include: developments of the liquid drop model (*50, 51, 102*), calculations based on dependence of fission barrier penetration on asymmetry (*34*), the effect of nuclear shells (*52, 79, 81*), the determinations of the fission mode by level population of the fragments (*18, 33, 84*), and finally the consideration of quantum states of the fission nucleus at the saddle point (*15, 108*). All these approaches require a mass formula whereby the masses of the fission fragments far removed from stability may be determined. The lack of an adequate mass formula has hindered the development of a satisfactory theory of fission. The fission process is highly complex and it is not surprising that the present theories fall short of a full explanation.

For the thermal neutron fission of U^{235}, the process can be represented by the following equation:

$$U^{235} + n \rightarrow U^{236*} \rightarrow Z_1A^{m_1} + Z_2B^{m_2} + \nu(n) + 173 \text{ Mev}, \qquad (14)$$

where $Z_1 + Z_2 = 92$, and $m_1 + m_2 + \nu(n) = 236$.

The primary fission products A and B are formed with a proton-to-neutron ratio which is less than that for stable nuclei of the same mass. The fragments are therefore proton deficient and undergo a series of β^--decays in a chain until they attain stability. Each mode of fission, therefore, leads to two such chains. For example, mass chains 133 and 101 may be complementary masses in the above fission process where ν the average number of neutrons emitted per fission is 2. In this case, the mass chains are as follows

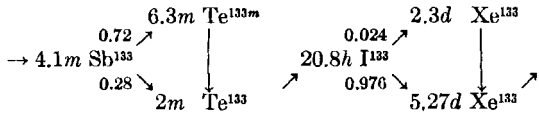

(15)

$$\rightarrow 14.6m\ Mo^{101} \rightarrow 14.3m\ Tc^{101} \rightarrow \text{stable } Ru^{101}$$

For the fission of each heavy nucleus, it is important that we have as much information as possible about the fission products, for both practical and theoretical reasons. In general, we wish to identify all the products, to determine their genetic relations one to the other, to determine their nuclear properties, half-lives, neutron cross sections, etc., and finally, to determine the fission yields of the various nuclides (independent yields) and of the various mass chains (cumulative yields or total of the independent yields along a chain). The yield is defined as the percentage probability per fission that a given nuclide or mass chain will be formed.

Whereas the yields of the individual nuclides give the charge distribution for fission fragments of the same mass, the cumulative yields or chain yields give the probability of the various modes of fission or mass distribution for a given fission process. It has been shown (*38, 87*) in studies of the distribution of nuclear charge in fission that in most cases the last two members of a fission product chain are formed almost exclusively from the decay of precursors, and only a small fraction of the yields of the last two members result from direct formation from primary fission fragments (prompt neutron emission only). Therefore, a fission yield measured for any of the later members of a mass chain, particularly for the stable or long-lived end products, usually represents the total yield of that chain. Independent yields found for shielded nuclides (nuclides immediately following a stable isotope in a mass chain) although of considerable interest

from the point of view of charge distribution (see Section V.F) are, in general, very small and add little to the total chain yield.

B. Relative Mass Chain Yields

1. Relative Yields; the Mass Spectrometric Method

It was clear from the time of the first fission product studies that the mass spectrometer would eventually be used in separation problems, mass identification, and isotope abundance measurements. However, the early work on fission products involved very small samples of material and only radiochemical methods were considered sensitive enough to identify and follow the radioactive isotopes. In 1945, Thode and Graham (*104*) succeeded in obtaining mass spectrograms of the xenon and krypton isotopes formed in the thermal neutron fission of U^{235}.

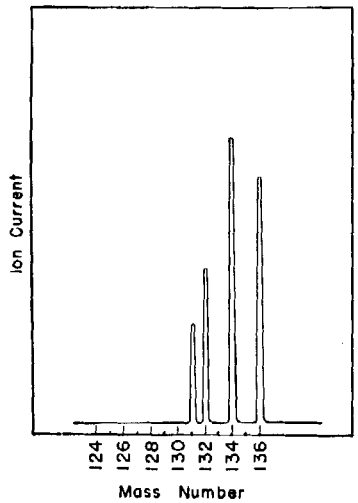

Fig 4. Mass spectrogram of fission product xenon from neutron-irradiated U^{235} (*104*).

These early spectrograms shown in Figs. 4 and 5 were obtained with a 180° gas-type mass spectrometer, using fission gas samples of 0.1 to 1 mm^3 in volume at N.T.P. (*105*). The importance of this method of investigating fission products was immediately recognized. Stable and long-lived isotopes of xenon and krypton which are end products of fission chains, were identified for the first time. Since these products were extracted from the uranium several years after the neutron irradiation and since the precursor nuclides were known to be all relatively short-lived, it could be assumed that the

total yield of each mass chain would be in the form of these stable isotopes. The relative abundances of these isotopes, therefore, gave directly the relative yields of the respective mass chains. Many of these cumulative yields have been obtained by measuring, with radiochemical methods, the relative number of atoms of iodine in the various radioactive chains. However, to obtain the yields in this manner, the data must be corrected for the half-lives of the isotopes measured and for the relative counter efficiencies for radiations of different energies. Because corrections of this kind are difficult and uncertain, the early radiochemical yield data were uncertain by at

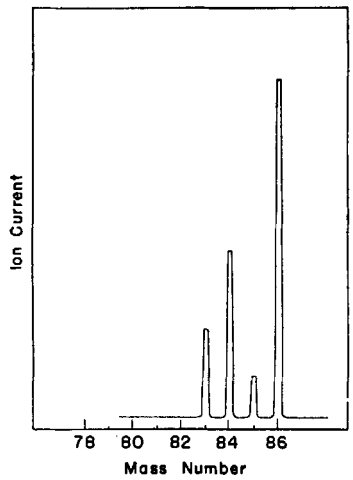

FIG. 5. Mass spectrogram of fission product krypton from neutron-irradiated U^{235} (*104*).

least $\pm 20\%$. Even today, with modern counting techniques, yields determined by radiochemical methods are rarely better than $\pm 5\%$. The mass spectrometer, on the other hand, provides a method of determining directly the relative yields of a large number of mass chains for each element investigated with an accuracy of 1.0% or better. In the case of the xenon and krypton isotopes, relative yield data were provided in the first instance for 8 mass chains (*104*).

2. Fission Yields and Problems of Chain Branching

a. Independent isomers (Kr^{85}). The identification of Kr^{85} which had a low yield relative to masses 84 and 86 in fission gas samples 1–2 yr old (Fig. 5) was of particular interest (*104*). Prior to 1945, the only Kr^{85} isomer known had a 4.5-hr half-life, an activity first noted by Snell (*98*),

while studying the (d,p) reaction on krypton. In 1945, Hoagland and Sugarman (*53*) found an activity with a minimum half-life of 10 yr when investigating the gaseous activities in fission products. They were able to show that this was due to an isotope of krypton and assigned it either to Kr^{85} or Kr^{87}. The long-lived isotope of krypton revealed in the mass spectrograms of gaseous fission products showed the definite existence of a long-lived isotope of krypton at mass 85 and hence an isomer of the known 4.5-hr krypton of that mass. By following the decrease of this isotope over a period of a few months, Thode and Graham were able to show that it decayed with a half-life of about 9.4 yr (*104*). A more recent mass spectrometric measurement made with samples 1–8 yr in age, an elapsed time of the same order as that of the half-life, gives the more accurate value of 10.27 ± 0.2 yr (*112*). The krypton isotope at mass 85 has therefore two isomeric states, a long-lived one with a half-life of 10.27 yr and a short-lived one with a 4.4-hr half-life. Since the shorter-lived isomer will have completely decayed before the fission gases were extracted from the uranium samples, the mass spectrometer results of Fig. 5 will indicate only the yield of the 10.27-yr isomer. The low yield found for this isomer indicated a chain branching with a large portion of the short-lived isomer decaying directly to Rb^{85} and only a small part, 25%, decaying first to the 10.27-yr isomer or ground state of Kr^{85}. By making the assumption that mass yields for chains 83, 84, 85, and 86 fall on a smooth curve (Fig. 5), the total yield of the 85 mass chain may be determined. This procedure, used by Wanless and Thode (*113*) gave a branching ratio for the decay of Kr^{85} of 0.29, the 4.4-hr Kr^{85m} decaying 77.5% directly to stable Rb^{85} and 22.5% through the 10.27-yr Kr^{85} isomer as follows (*61*):

$$\begin{array}{l} \qquad\qquad\qquad\quad 4.4h\ \ Kr^{85m} \qquad\quad \searrow 0.775 \\ 40s\ Se^{85} \rightarrow 3m\ Br^{85} \nearrow \qquad\quad \downarrow 0.225 \qquad\quad \text{stable } Rb^{85} \\ \qquad\qquad\qquad\quad 10.3y\ Kr^{85} \qquad\quad \nearrow \end{array} \tag{16}$$

The value of this branching ratio measured directly from β^--decay data is 0.30 (*11*) whereas a direct measure of the fission yields of Kr^{85} and Rb^{85} using mass spectrometry and isotope dilution gave a value of 0.28 (*13*). The assumption that the Kr^{85} yield falls on a smooth mass yield curve in the case of the thermal neutron fission of U^{235} therefore appears to be justified.

b. Delayed neutron emitters. All fission yield determinations must take into account chain branching due to delayed neutron activities and neutron capture processes. Both Kr^{87m} and Xe^{137m} each with one neutron more than a closed shell (51 and 83, respectively) are instantaneous neutron emitters (*99*) and lead to chain branching as follows (*61*):

$$
\begin{array}{ccccc}
 & & & & Kr^{86} + n \\
 & & & & \uparrow \\
17s\ Se^{87} \rightarrow 55s\ Br^{87} & \nearrow & Kr^{87m} & \nearrow & 5 \times 10^{10}y\ Rb^{87} \\
 & \searrow & 17.8m\ Kr^{87} & \nearrow & \\
 & & Xe^{136} + n & & \\
 & & \uparrow & & \\
24s\ I^{137} & \nearrow & Xe^{137} & \nearrow & 2.57m\ Ba^{137m} \\
 & \searrow & 3.9m\ Xe^{137} & \nearrow 29y\ Cs^{137} & \searrow \text{stable } Ba^{137}
\end{array}
\tag{17}
$$

Because of the delayed neutron activities of 55 sec and 24 sec which are derived from β^--decay half-lives of Br^{87} and I^{137}, respectively (the neutron emission is instantaneous and follows the β^--emission), the two mass chains 86 and 136 gain in yield at the expense of the 87 and 137 chains, respectively. However, in general, these effects are small, amounting to a few percent of the yield of a chain at most.

c. Neutron capture processes. Neutron capture processes, however, can lead to a large increase in the yield of one chain at the expense of the chain one mass unit lower, and, of course, the extent of this chain branching will depend upon neutron capture cross sections of the nuclide in question and the conditions of irradiation.

In general, only nuclides with high capture cross sections lead to appreciable chain branching at moderate neutron fluxes. An important example of a "pile poison" or a high neutron absorber is the 9.2-hr Xe^{135} which has been discussed in Section IV. In this case, the "burn up" is appreciable even at fluxes of the order of 5×10^{12} neutrons/cm^2/sec. The neutron capture process in the 135 mass chain is indicated below (*61*):

$$
\begin{array}{ccccc}
 & & 15.3m\ Xe^{135m} & & \\
 & & \downarrow & & \\
Te^{135} \rightarrow 6.7h\ I^{135} & \nearrow & 9.2h\ Xe^{135} & \nearrow & 2.6 \times 10^6y\ Cs^{135} \\
 & \searrow & \downarrow +n & & \\
 & & \text{stable } Xe^{136} & &
\end{array}
\tag{18}
$$

Because of this capture process, the mass spectrometer abundance data for the xenon isotopes from fission will show a high yield value of the 136 mass chain, and similar data for the cesium isotopes will show a correspondingly low value at mass 135. The percentage increase in the Xe^{136} yield due to this neutron capture process can, of course, be calculated, provided we have accurate information concerning the number of fissions per second, the half-lives of I^{135} and Xe^{135}, the neutron capture cross section σ of Xe^{135} at the neutron temperature of the irradiation, and, finally, the length of the irradiation period (Section IV).

d. Relative cumulative yields of isotopes of xenon and krypton from U^{235} + n fission. To obtain accurate relative yields, however, it is far better to avoid any corrections for neutron capture processes by irradiating sam-

ples for investigation at low fluxes, where such processes are negligible. The early mass spectrometer yield determinations of the isotopes of xenon and krypton for the thermal neutron fission of U^{235} were repeated with this in mind (*113*). Fission gases for study were extracted from uranium irradiated in the thermal column of a reactor at fluxes of the order of 10^{10} neutrons/cm^2/sec.

The relative abundances of the xenon and krypton isotopes obtained with these samples provide the best relative yields of mass chains ending in these isotopes for the thermal neutron fission of U^{235}. Table I gives this

TABLE I

FISSION PRODUCT XENON AND KRYPTON ISOTOPE ABUNDANCES FOR URANIUM IRRADIATED IN NRX THERMAL COLUMN[a]

Isotope	Atom abundance (%)	Absolute fission yield[b] (%)
Kr^{83}	14.10	0.557
Kr^{84}	25.93	1.02
Kr^{85} 10.27-hr	7.59	0.300
Kr^{86}	52.38	2.07
Xe^{131}	13.42	2.93
Xe^{132}	20.08	4.38
Xe^{134}	36.91	8.06
Xe^{136}	29.59	6.46
[c]Xe^{133} 5.27-day	Xe^{131}/Xe^{133} (0.443)	6.59

[a] Fission product isotope abundances (*14*, *113*).

[b] Xe^{131}/Xe^{133} ratios (*14*).

[c] Absolute yield Cs^{133} (6.59%) (*90*), also Xe^{133} yield (6.62%)(*60*).

relative yield data normalized to 6.59% at Xe^{133}. This latter absolute yield was determined both at Xe^{133} (*60*) and Cs^{133} (*90*) by methods described in Section V.C, and in addition the partial yield curves for krypton and xenon were tied together by an absolute determination of the number of xenon and krypton atoms by means of the isotope dilution technique (Section I).

3. *The Cumulative Yield of 5.27-Day* Xe^{133}

Mass spectrometer yield determinations are not limited to stable and long-lived end products of fission chains. In 1950, Macnamara, Collins, and Thode (*77*) found it possible to extract fission gases from irradiated uranium disks without a long "cooling" period and were able to determine the yield and half-life of Xe^{133}. The mass spectrograms obtained were similar to those given in Figs. 4 and 5, except for the appearance of Xe^{133}, and, of course, the Xe^{131} abundance was low since the 8-day I^{131} precursor had not fully decayed. The fission yield of the 133 mass chain for U^{235} fission is calculated

from the mass spectrometer abundance ratio of Xe^{133} to Xe^{134} obtained after an irradiation time t, a "cooling time" t_1, and at a time t_2 after extraction of the fission gases.

The two mass chains being compared are as follows:

$$\begin{array}{l} 0.8m\ Sb^{134} \rightarrow 44m\ Te^{134} \rightarrow 52.5m\ I^{134} \rightarrow \text{stable } Xe^{134} \\ 4.1m\ Sb^{133} \begin{array}{l} \nearrow 63m\ Te^{133m} \\ \searrow 2m\ Te^{133} \end{array} \begin{array}{l} \downarrow \\ \nearrow \end{array} 20.8h\ I^{133} \begin{array}{l} \nearrow 2.3d\ Xe^{133m} \\ \searrow 5.27d\ Xe^{133} \end{array} \begin{array}{l} \downarrow \\ \nearrow \end{array} \text{stable } Cs^{133} \end{array} \tag{19}$$

As the period of "cooling" is long compared to the half-lives of the Xe^{134} precursors, the total mass 134 chain will decay to Xe^{134}. Therefore, the total number of Xe^{134} atoms at time of analysis is given by:

$$N_{Xe^{134}} = fY_{134}t, \tag{20}$$

where Y_{134} is the yield of the 134 mass chain and f the neutron flux during irradiation time t. The ratio of the total number of Xe^{133} atoms to the total number of Xe^{134} atoms at the time of analysis is therefore given by the equation:

$$\begin{aligned} \frac{N_{Xe^{133}}\,[\text{at } t_2]}{N_{Xe^{134}}} = \frac{\exp(-\lambda_2 t_2)}{Y_{Xe^{134}}t}\, Y_{133} \Bigg\{ \Bigg[\frac{1 - \exp(-\lambda_1 t)}{\lambda_2 - \lambda_1} \Bigg] \\ \times \Bigg[\exp(-\lambda_1 t_1) - \exp(-\lambda_2 t_1) + \frac{\exp(-\lambda_2 t_1)}{\lambda_2} \Bigg] \\ \times \Bigg[1 - \frac{\lambda_2 \exp(-\lambda_1 t) - \lambda_1 \exp(-\lambda_2 t)}{\lambda_2 - \lambda_1} \Bigg] \Bigg\}, \end{aligned} \tag{21}$$

where λ_1 and λ_2 are the decay constants of I^{133} and Xe^{133}, respectively.

The measured mass spectrometer ratio of Xe^{133}/Xe^{134} at t_2 (time of analysis) which may be equated to the left side of the equation, therefore makes possible the calculation of the yield Y^{133} of the mass chain.

Since the independent yield of Cs^{133} will be negligible the total yield obtained for the 133 mass chain should be the same whether measured at Xe^{133} or Cs^{133}. The Xe^{133} cumulative yield therefore provides a link between the relative yields of 8 mass chains ending in stable and long-lived isotopes of xenon and krypton and of the 3 mass chains ending in stable and long-lived isotopes of cesium.

4. Relative Yields Over Entire Mass Range

The mass spectrometric method of fission product yield measurements can be applied to the entire mass range of fission products. Inghram *et al.* (*55*) investigated fission products in the rare earth region and showed how the partial yield curves obtained from isotope abundance measurements for the various elements can be fitted together by the method of stable

isotope dilution. This method has been used extensively in the analysis of fission products (*13, 14, 44, 59, 60*), and as described in Section I, makes possible the determination of the absolute number of atoms of each nuclide in a mixture of fission products and extends the mass spectrometric method of yield determinations to the whole mass range.

One important feature of the mass spectrometric method of fission yield determinations is the ease with which a large number of mass chains may be investigated at the same time for a mixture of fission products from a single irradiation. Since ions for the various elements are emitted from a sample on a hot filament at different temperatures, isotope abundance measurements of a number of elements may be made on a single sample without chemical separation. It is, therefore, possible to obtain a large body of yield data for a particular fission process with high relative accuracy ($\pm 1\%$).

Fission yields of the stable and long-lived isotopes of xenon, cesium, barium, cerium, neodymium, samarium, krypton, rubidium, strontium, zirconium, molybdenum, ruthenium, have been measured mass spectrometrically for the thermal neutron fission of U^{235} (*40, 61, 90*), U^{233} (*4, 31, 61, 82, 100*), and Pu^{239} (*32, 61, 66, 124*). In addition, the relative yields of the xenon and krypton isotopes produced in the fast neutron fission (fission spectrum neutrons) of U^{238} and Th^{232} (*64, 113*) have been determined.

C. Absolute Mass Chain Yields

1. Total Yields Normalized to 100%

The relative yields of the isotopes of the aforementioned (Section V.B.4) twelve elements that can be measured mass spectrometrically give reliable yields of about 43 mass chains. These, taken together with a number of yields determined radiochemically, give essentially the whole mass yield curve, which may be normalized to 100% in order to obtain absolute yields for the various mass chains. This procedure is used when mass chain yields for most of the chains of appreciable yield for either the light or heavy fragments are known. Absolute yields good to $\pm 3\%$ have been obtained in this way.

2. Direct Measurement of Absolute Yield

To obtain absolute yields directly, it is necessary to determine, not only the absolute number of atoms of a nuclide produced in fission, but, also, the total number of fissions. The determination of the number of fissions in a sample of a fissile element irradiated with neutrons is a most complex problem and cannot be discussed in detail here. In general, the number of

fissions can be determined by measuring the change in the B^{10}/B^{11} ratio in a BF_3 flux monitor irradiated simultaneously in the same neutron flux as the fission sample. Conversion to the number of fissions is then effected by the use of the known ratio of B^{10} absorption cross section to the fission cross sections (*91*). Cobalt and samarium have also been used as flux monitors. In the case of the cobalt, the amount of Co^{60} formed from a known amount of cobalt can be determined by ionization chamber measurements, using standard cobalt sources for comparison. In the case of the samarium, the change in Sm^{150}/Sm^{149} ratio is determined by mass spectrometry.

In the determination of the number of fissions in an irradiated sample by the use of flux monitors, account must be taken of the flux depression in the sample due to self-shielding to obtain an effective flux. Also, the capture cross sections of the monitors and the fission cross sections of the sample are neutron energy dependent. It is, therefore, necessary to know the energy distribution of the neutrons or the neutron temperature and to determine effective cross sections (Section IV). This can be done by using two monitors such as cobalt and samarium, the one monitor being used to determine the neutron temperature corresponding to the neutron distribution as described by Fritze *et al.* (*35*).

3. Summary of Absolute Yield Determinations

Katcoff (1958) has prepared tables of fission product yields from low-energy neutron-induced fission of U^{235}, Th^{232}, and Pu^{239} (*61*). In the compilation of these tables he has given first priority to mass spectrometric data since these are more accurate ($\pm 3\%$) than most radiochemical data ($\pm 10\%$). Since these tables were prepared, the absolute yields of some 43 mass chains from the thermal neutron fission of Pu^{239} have been redetermined using mass spectrometric methods (*29, 35*). These yields are considered accurate to better than 1% on a relative basis and better than 3% on an absolute basis. The earlier determinations have been shown to be in considerable error because of incomplete extraction of fission products from PuO_2.

4. Interpretation of Mass Yield Curves for $U^{235} + n$ *and* $Pu^{239} + n$ *Fission*

The mass yield data for the thermal neutron induced fission of U^{235} and Pu^{239} are plotted in Figs. 6 and 7, respectively. In each case the mass yield curve is folded over so that complementary masses fall together assuming that 2.5 neutrons ($U^{235} + n$) and 3 neutrons ($Pu^{239} + n$) are emitted per fission. This means that the sum of the corresponding masses totals 233.5 and 237, respectively.

A complete mass yield curve makes it possible to calculate the total

number of neutrons, ν, released in a fission process. For example, in the neutron-induced fission of Pu^{239}

$$\nu = 240 - 2\left(\frac{\sum \text{mass} \times \text{yield}}{\sum \text{yield}}\right). \tag{22}$$

From the data of Fickel and Tomlinson (*29*) a value of 2.80 ± 0.08 is obtained assuming an absolute accuracy of $\pm 3\%$ for the measured fission yields. This is in agreement with the world-accepted value of 2.90 (*114*).

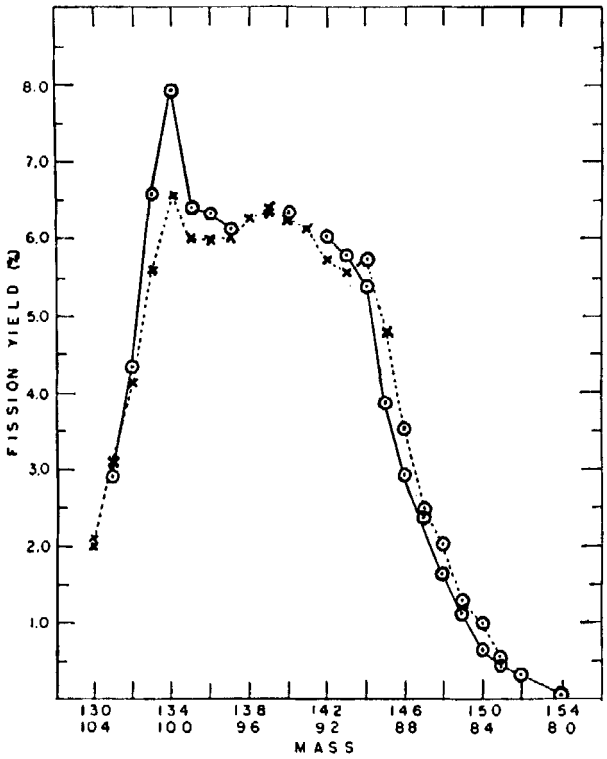

FIG. 6. Comparison of the light and heavy mass yields in the thermal neutron fission of U^{235} (*91*). KEY: —, heavy; ---, light.

A more detailed consideration of Fig. 7 shows that the corresponding mass chains in the light and heavy groups have equal yields in the mass ranges 138–154, 83–99, indicating the emission of three neutrons per fission on the average for modes of fission in this region. Although there is a dearth of measured fission yields in the 96–118 and 118–131 mass region, the displacement of the curves in Fig. 7 of approximately 1 mass unit suggests that on the average only 2 neutrons are emitted per fission in modes of

fission leading to these masses. Finally, in the mass region 132–138, 105–99, the yields of the corresponding masses in the light and heavy regions do not correspond at all. This is the region of the "fine structure" in the neighborhood of the 82 neutron shell.

In the case of neutron-induced fission of U^{235} there is again good correspondence between fission yields for the light and heavy fragments in the 138–154, 83–99 mass regions (Fig. 6). The correspondence occurs, however, for the average neutron emission of 2.5 per fission. As in the case of the Pu^{239}

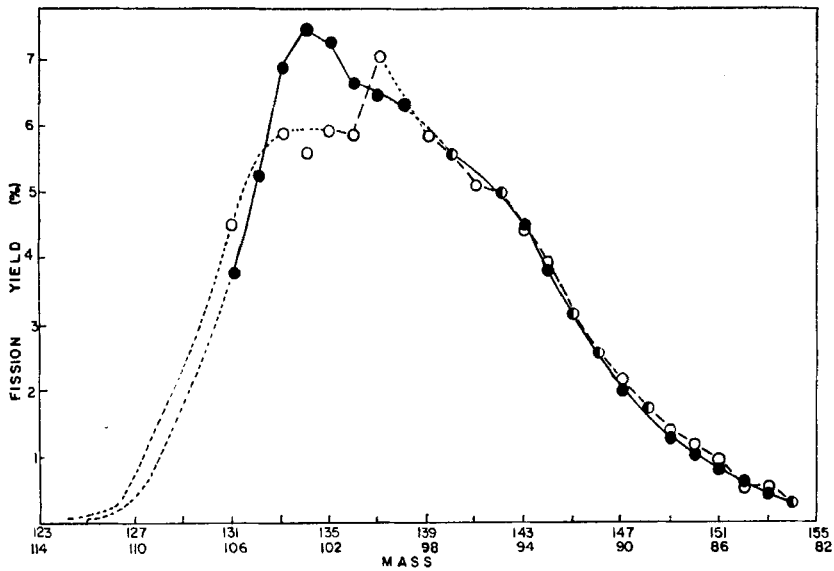

FIG. 7. Comparison of the light and heavy mass yields in the thermal neutron fission of Pu^{239} (*27*, *29*). KEY: ●—●, heavy masses; ○---○, light; ◐, light and heavy.

fission, the curves appear to be displaced in the mass region 117–131 and 103–117 indicating correspondence of yields for light and heavy fragments for the emission of 2 neutrons per fission on the average rather than 2.5 neutrons. Again, there is poor correspondence between the light and heavy mass yields in the mass region where fine structure occurs. These yield curves have suggested another possible explanation of the "fine structure" discussed in the next section.

D. FINE STRUCTURE IN MASS YIELD CURVE

1. Fine Structure in 82 Neutron Shell Region

The early fission yield data obtained by radiochemical methods, although only good to ±10% at best, did give the familiar double hump mass

yield curve and showed that the fission process was asymmetric with the most probable modes of fission grouped around masses 95 and 140. Within the limits of the radiochemical determinations, a smooth curve could be drawn through the yield values for the various masses. However, the first mass spectrometric investigations of fission products showed up irregularities and established the existence of "fine structure" in the mass yield curve (*104*). In particular, the yield of Xe^{134} is high relative to the two adjacent masses and there is a sharp peak at masses 133 and 134 in the mass yield curve for $U^{235} + n$ fission (Fig. 4).

It is interesting to note that this fine structure falls in the neighborhood of the 82 neutron shell. Four or five mass chains in this range each have one nuclide with 82 neutrons with a significant independent yield, and in the case of the 134 mass chain, this nuclide Te^{134} is the most probable member of the chain according to the Coryell, Glendenin postulate of charge distribution for a given mass in fission (see Section V.F).

Glendenin (*37*) attempted to explain the high yields of the 133 and 134 mass chains by assuming that nuclei with 83 neutrons (which has already emitted the usual number of prompt neutrons) would have a high probability of "boiling off" a prompt neutron to form the most stable 82 neutron configuration rather than emit β^- or γ rays as in the ordinary case. According to this scheme, the 134 mass chain would be increased by the reaction

$$Te^{135}\ (83\ \text{neutrons}) \rightarrow Te^{134}\ (82\ \text{neutrons}) + n; \tag{23}$$

and decreased by the reaction

$$Sb^{134}\ (83\ \text{neutrons}) \rightarrow Sb^{133}\ (82\ \text{neutrons}) + n.$$

If Te^{135} has a higher independent yield than Sb^{134}, then the 134 chain will gain more than it loses by this mechanism and the Xe^{134} yield will be high.

Although reaction (1) should be greater than reaction (2) on the basis of the simple theory of "charge distribution" in fission, this mechanism cannot explain the observed fine structure. Wiles *et al.* (*121*), therefore, postulated that in addition to the Glendenin mechanism high yields must result from a structural preference for isotopes with 82 neutrons in the primary fission act. Glendenin *et al.* (*39*) reached a similar conclusion after observing a high yield at mass 100, the complementary fragment to the 134 mass chain (Fig. 6).

Investigations of the xenon isotope yields in the neutron-induced fission of U^{233} (*31*), U^{238} (*113*), Pu^{239} (*32*), and Pu^{241} (*36*) have also been carried out. In all cases, there is evidence of some increased yield in the xenon mass range. The sharpness of the peak at mass 134 varies considerably, however, and in the case of $U^{233} + n$ fission, there is little evidence of fine structure

from the xenon isotope yields alone. The entire fission yield curve for $U^{233} + n$ fission, however, does indicate an increased yield in this mass range spread out over a larger number of mass chains.

The complete fission yield curve obtained for the neutron-induced fission of Pu^{239} has suggested another explanation of the fine structure in the mass yield curve in the 132–136 mass range (*27*, *29*). Since the folded over fission yield curve of Fig. 7 discussed in Section V.C.4 indicates correspondence of yields of the light and heavy fragments for the emission of 3 neutrons on the average in one region of mass division and 2 neutrons in another, there must be a mass region in which a transition occurs.

Fickel and Tomlinson (*27*) have suggested that an increased stability of primary fragments in the heavy mass region, perhaps those having either 82 neutrons or 50 protons, may cause a decrease in neutron emission at this point. Such a decrease in neutron emission would cause a bunching up of yields such as those found in the 131–136 mass range. The total effect would be to increase the yields in the 131–136 mass range by one half of the yield of a single mass chain in this region (3% of fission). A corresponding decrease in the yields could occur in the 100–106 range by approximately the same amount. It is seen from Fig. 7 that the total yield discrepancies in these two complementary mass regions do differ by about 6%. The complete mass yield curves obtained for the neutron-induced fission of U^{235} suggest a similar explanation of the fine structure in the mass yield curve at xenon (masses 131–136).

This latter explanation of fine structure is a plausible one. However, complete fission yield curves for the neutron-induced fission of other fissile nuclides are needed to add further light on this problem.

2. Fine Structure in the 50 Neutron Shell Region

It is perhaps significant that irregularities in the mass yield curve occur also in the region of the 50 neutron shell. These irregularities appear in the yields of mass chains ending in stable isotopes of krypton. Figure 8 shows the krypton yields for Th^{232} (*64*), U^{233} (*31*), U^{235} (*14*), and U^{238} (*113*) obtained mass spectrometrically. It is apparent that the mass yield curve in this region moves to higher yields as the mass of the fissile nuclide decreases. This indicates that the mass yield curve for the light fragments is actually displaced. The mass displacement of these curves, for a fixed fission yield, is approximately equal to the mass difference between the fissile nuclides. This implies that the heavy fragment portion of the mass yield curve remains at a relatively constant position. A closer examination shows a fine structure at masses 84 and 85. It has been suggested that since the relative yields of the krypton isotopes may be determined mass spectrometrically with an accuracy of 1% and a precision of 0.1%, there is little question

about the existence of fine structure effects which amount to a 40% change in the isotope ratio.

The high 84 yield in all four cases probably arises from a preference for this chain in the original fission process or cross chain branching from the 85 mass chain. The behavior of the 85 yield depends on the fissile nuclide and is high for U^{233}, normal for U^{235}, and low for Th^{232} and U^{238}. The deviation of the 85 yield from the smooth mass yield curve can be correlated with the Z/A value of the fissile nuclide. This suggests that a branching

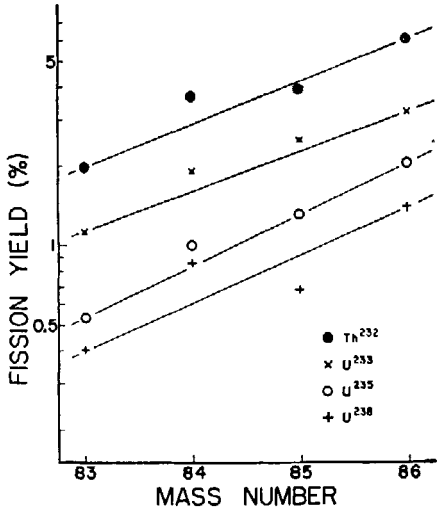

FIG. 8. The krypton yields for neutron-induced fission of Th^{232}, U^{233}, U^{235}, and U^{238} (*64*).

(neutron emission) may occur in the 85 chain since the independent yield of such a prompt neutron emitter would be related to the Z/A value of the fissile nuclide. The nuclide in question must have a fairly high independent yield and possess a low threshold for neutron emission. Kennett and Thode (*64*) point out that these conditions are fulfilled by $_{34}Se^{85}$ which has 51 neutrons, one more than a closed shell. As pointed out by Glendenin (*37*) the loss of the loosely held 51 neutron would probably occur only where the nuclide was formed as a fission fragment (after the usual prompt neutron emission) in a highly "excited" state. Since the fractional yield of the mass chain occurring at Se^{85} (primary yield) will depend on Z/A, any chain branching at this nuclide should show about the same percentage effect for U^{238} and Th^{232}.

3. Fission Products from Several Fission Processes

Because of the fine structure in the mass yield curve in the 131–136 mass range, ratios of the xenon isotopes in this region vary markedly from

one fission process to another. This makes possible a convenient method of unraveling a mixture of fission products produced from several different fission processes.

The early studies of fission products from neutron-induced fission of U^{235} were carried out with samples of natural uranium irradiated with "pile" neutrons which were not completely thermalized. A comparison of the mass spectrograms of the xenon isotopes extracted from one of these samples with those extracted from uranium depleted in U^{235} indicated a 14% contribution from U^{238} fission in the natural uranium samples (*113*). Also, a sample of natural uranium irradiated in a fast reactor showed a 60% contribution from U^{238} fission. The mass spectrometric method can be conveniently used to measure the fission contribution from U^{238} and U^{235} in fuel elements of reactors where natural or enriched U^{235} fuels are used.

E. Neutron-Induced and Spontaneous Fission in Nature

Soon after the discovery of fission, Petrzhak and Flerov (*92*) demonstrated with ionization chambers that uranium undergoes fission spontaneously and emits neutrons in the process. Later, Segre (*95*) used separated isotopes of uranium and showed that U^{238} has a spontaneous fission rate of about 23 times that of U^{235}, the half-lives for spontaneous fission of U^{238} and U^{235} being 8.04×10^{15} yr and 1.87×10^{17} yr, respectively. These results suggested the presence of fission products in uranium minerals. In 1950, xenon and krypton fission products were identified in old uranium minerals using mass spectrometric methods (*75*). The patterns of xenon and krypton isotopes found indicated an asymmetric mass yield curve similar to that obtained in the neutron fission of U^{235} and U^{238}.

1. *Spontaneous Fission of* U^{238} *and Neutron Fission of* U^{235}

There were, however, certain marked differences. First, the mass yield curves in the xenon and krypton mass ranges were steeper for natural fission. Since there is much less energy available for spontaneous fission than for neutron fission, the process is expected to be more selective (steeper curves). This was considered strong evidence that spontaneous fission of U^{238} is involved in natural fission. Second, the abnormally high yields found at masses 133 and 134 (fine structure in the mass yield curve) in the neutron fission of U^{235} are shifted toward the lower masses for natural fission which is the same direction of shift found between neutron fission of U^{235} and neutron fission of U^{238}. Third, the xenon-to-krypton ratio was found to be much higher in natural fission gases. From this and other evidence, Macnamara and Thode (*75*) concluded that at least a large part of the fission gases in uranium minerals resulted from the spontaneous fission of U^{238}.

Later, it was shown that both neutron fission of U^{235} and spontaneous

fission of U^{238} occur in nature (*30, 117*) and that the xenon and krypton isotope pattern found is a composite for the two processes. The fission isotope patterns of xenon and krypton were found to vary from one sample to another, depending on the proportion of the two fission processes which have taken place. Since the mass 129 chain yield is about 1.0% for the neutron fission of U^{235} and was found to be very nearly zero for the spontaneous fission of U^{238}, the yield of this isotope was taken as an index of the proportion of neutron fission of U^{235} and spontaneous fission of U^{238} which has occurred in a given mineral. Several minerals investigated were found to contain less than 0.02% Xe^{129}, indicating that at least 98% of the fission gas was due to the spontaneous fission of U^{238}. Other samples showed up to 25% neutron fission of U^{235}. There are, of course, two sources of neutrons for this process, spontaneous fission and (α,n) reactions on light elements.

2. Absolute Yields

a. Spontaneous fission of U^{238}. Recently, absolute cumulative yields of the xenon and krypton fission products from six uranium minerals were determined mass spectrometrically, using isotope dilution techniques (*126*). The uranium ores were crushed and sieved to about 100 mesh and finally concentrated to a density greater than 3 by gravitational separation with diiodomethane. A homogeneous aggregate of uranium mineral concentrate was produced by this procedure suitable for the extraction and analysis of the fission gases. Greater than 99.5% of the fission gases was released by heating the mineral concentrate in a molybdenum crucible in a vacuum induction furnace over a period of 12 hr at 1300°C. The absolute yield calculation for the spontaneous fission of U^{238} depends on the independent determination of the number of spontaneous fissions which have taken place and the number of atoms of a given fission product which has been formed from this process.

The total number of U^{238} atoms which have undergone spontaneous fission in a mineral sample since deposition are calculated from the U^{238} content, the age, and the rates at which the U^{238} nucleus decays by alpha emission and by spontaneous fission according to the relation:

$$N = W\lambda_f/\lambda_\alpha(e^{\lambda_\alpha T} - 1); \tag{24}$$

where W is the present number of U^{238} atoms in the mineral sample; λ_f, the U^{238} spontaneous fission decay constant [$8.62 \pm 0.30 \times 10^{-17}$/yr (*95*)]; λ_α, the U^{238} decay constant [$= 1.54 \times 10^{-10}$/yr (*65*)]; T, the period during which fission products accumulated, assumed to be given by the lead isotope age measurement.

The total number of atoms of each fission product xenon and krypton isotope in the mineral sample was determined by means of mass spectrom-

etry and the isotope dilution technique discussed in Section I. In this connection, known quantities of the tracer isotopes Xe^{128}, Kr^{80}, and Kr^{82}, prepared by the neutron irradiation of iodine and bromine in the NRX reactor at Chalk River, were added to the impure fission gases liberated from the uranium mineral concentrate. Finally, the fraction of the fission gas in each mineral sample which resulted from the spontaneous fission of U^{238} was obtained from a breakdown of each natural fission gas sample into its various fission components. This analysis makes use of the known relative abundances of the xenon and krypton isotopes for the various possible fission processes separately and a comparison of these with the relative abundances obtained for the fission gases extracted from the various minerals. As mentioned in Section V.D.3, the ratio of the xenon and krypton isotopes in fission product gases varies markedly, depending on the nature of the fission processes because of the fine structure which occurs in this region.

b. Neutron fission of U^{238}. A preliminary analysis of the data showed that it was not possible to separate satisfactorily the six mineral isotope patterns into a U^{235} neutron-induced component and a U^{238} spontaneous fission component. However, a satisfactory analysis was obtained when a third component, U^{238} neutron-induced fission, was considered along with the two processes proposed earlier (*30*). Table II shows the breakdown obtained for the six samples investigated.

c. Proportion of neutron-induced fission. These results indicate that there is a correlation between the percentage of uranium in a mineral concentrate and the percentage of neutron fission. This relationship is shown in Fig. 9. The percentage of uranium in the mineral concentrate should be approximately equal to the percentage of uranium in the mineral itself, since most of the rock matrix was removed by gravitational separation with diiodomethane. It had been assumed earlier that the presence of the rare earth elements which have large thermal neutron absorption cross sections, is largely responsible for the low proportion of neutron fission in uraninites. The occurrence of U^{238} neutron fission in uranium minerals suggests much larger neutron energies than had been suspected and indicates that the rare earths have little effect on the amount of neutron fission in a uranium mineral. The fact that the Jahola Lake uraninite (high rare earths) and the Cinch Lake pitchblende, with equal uranium concentrations in the concentrates, have the same proportion of neutron fission, supports this conclusion.

d. Losses of fission gas from uranium minerals. Included in Table II are the ratios of the number of atoms of Xe^{136} determined to the number of fissions for each sample (spontaneous fission component only). These ratios expressed as percentages, can be interpreted as absolute yields only if no fission products have been lost from the mineral. The value obtained

TABLE II

FISSION-PRODUCT COMPONENTS IN NATURAL FISSION

Mineral	Cinch Lake	Jahala Lake	Beaverlodge Lake	Great Bear Lake	Eagle Mine	Belgian Congo
U^{238} Spontaneous fission (%)	95.86	96.15	91.82	81.65	80.42	68.65
U^{235} Neutron fission (%)	4.14	3.85	8.18	15.19	17.22	25.23
U^{238} Neutron fission (%)	0.00	0.00	0.00	3.16	2.36	6.12
$\frac{Xe^{136}\text{ (Spontaneous fission)}}{U^{238}\text{ (Spontaneous fission)}} \times 100$	6.30 ± 0.38	4.38 ± 0.18	1.59 ± 0.26	4.78 ± 0.23	3.21 ± 0.13	3.51 ± 0.17
Xe^{136} Loss (%)	0.0 ± 6.0	30.5 ± 6.6	74.8 ± 7.3	24.1 ± 7.1	49.0 ± 6.3	44.3 $\pm$ 6.5

for the Cinch Lake sample is in agreement with absolute yield estimates and therefore suggests that inert gas losses from this mineral have been small. If the "lead ages" are assumed to be the period during which spontaneous fission products accumulated, then the low yields of Xe^{136} for the other five minerals must be due to a loss of inert gas during geological time and these losses are given in Table II. If it is assumed that there was no

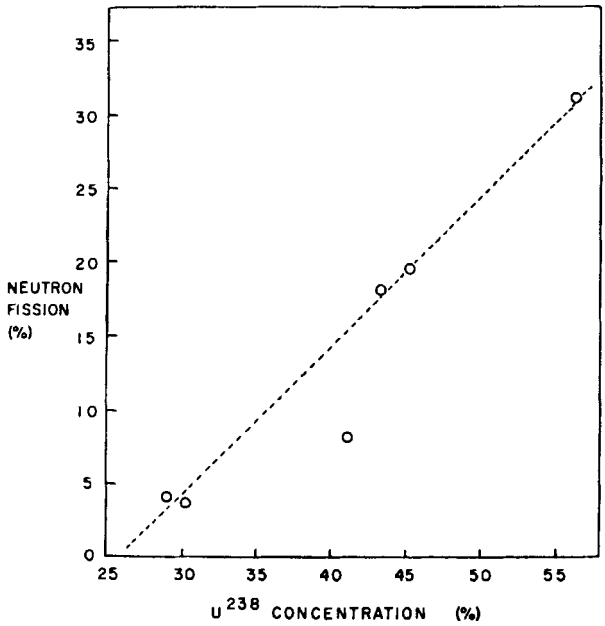

FIG. 9. Relation between the amount of neutron fission and uranium concentration in a uranium mineral or ore concentrate (*126*).

loss of fission gases from the Cinch Lake mineral since it was deposited, then the spontaneous fission yields obtained for this sample are absolute. The fact that there is little evidence of fractionation of the two rare gases, xenon and krypton, for this sample supports this assumption. In any case, the absolute yields of mass chains ending in stable isotopes of xenon and krypton from the spontaneous fission of U^{238} obtained for the Cinch Lake sample are minimum values.

3. Absolute Yield Data for the Spontaneous Fission of U^{238}

Recently, absolute yields of Mo^{99} and several iodine isotopes from spontaneous fission of U^{238} determined by radiochemical methods were reported by Parker and Kuroda (*89*) and Ashizawa and Kuroda (*5*). These yields, along with the absolute yields of the xenon and krypton isotopes obtained

for the Cinch Lake sample are given in Table III. The good agreement between the xenon and iodine yields at masses 131, 132, and 134 is in accord with the assumption that no fission product xenon and krypton had been lost from the Cinch Lake mineral. The large losses of rare gas fission products indicated by most of the uranium minerals prevents the general use

TABLE III

ABSOLUTE YIELDS IN U^{238} SPONTANEOUS FISSION

Mass	Element	Yield[a] (%)	Element	Yield (%)
83	Kr	0.0327 ± 0.0028		
84	Kr	0.122 ± 0.012		
85				
86	Kr	0.951 ± 0.057		
99			Mo	6.4 ± .5[b]
131	Xe	0.524 ± 0.031	I	0.4 ± .1[c]
132	Xe	3.63 ± 0.22	I	3.6 ± .4[c]
133			I	1.5 ± .3[c]
134	Xe	5.14 ± 0.31	I	5.2 ± .5[c]
135			I	5.1 ± .5[c]
136	Xe	6.30 ± 0.38		

[a] All data in this column were obtained by the authors.

[b] Parker and Kuroda

[c] Ashizawa and Kuroda

of accumulated rare gas fission products for age determinations. Nevertheless, the fractionation which accompanies loss should be a sensitive test of the validity of a "fission product age," that is, the period during which fission products have accumulated without loss.

F. INDEPENDENT FISSION YIELDS

For a complete understanding of the fission process, it is necessary to know both the charge and mass distribution of the fission fragments. Fission yield studies to date have been mainly concerned with mass distribution or the total or cumulative yields of a given mass. The question of charge distribution for a given mass involves the primary or independent yields of the fission fragments. The measurement of independent yields along a mass chain is very difficult with present techniques because of the very short half-lives of most members and the correction necessary for the decay rate and the production rate.

Attempts have been made to determine cumulative yields for some of the short-lived krypton and xenon isotopes by gas sweeping a solution of uranium undergoing fission. However, quantitative removal of inert gases

from solution was not achieved. Wahl (*109*) found that inert gases are quantitatively removed from barium or uranyl stearate and by utilizing well-designed experiments obtained values for the fractional cumulative yields of these short-lived inert gases.

1. Shielded Nuclides

For the most part, however, independent yield data are confined to about a dozen nuclides that are near stability and are shielded by stable or relatively long-lived isobars.

For example, in the mass chain

$$Sn^{130} \xrightarrow{\beta^-} Sb^{130} \xrightarrow{\beta^-} \text{stable } Te^{130}, \qquad I^{130} \xrightarrow{\beta^-} \text{stable } Xe^{130} \tag{25}$$

the independent yields of tin, antimony, and tellerium accumulate at stable Te^{130} and thus any yield of the shielded I^{130} is, therefore, the independent fission yield of that isotope. Since the primary fission fragments emit prompt neutrons, the independent yield $Y_{I^{130}}$ of I^{130} will be given by the equation:

$$Y_{I^{130}} = P_{I^{130}} f_0 + P_{I^{131}} f_1 + P_{I^{132}} f_2 + P_{I^{133}} f_3 + P_{I^{134}} f_4 + \ldots, \tag{26}$$

where $P_{I^{130}}$, $P_{I^{131}}$, $P_{I^{132}}$, $P_{I^{133}}$, and $P_{I^{134}}$ are the primary yields of I^{130}, I^{131}, I^{132}, I^{133}, and I^{134} at the instant of fission (before prompt neutrons are emitted), and f_0, f_1, f_2, f_3, and f_4 are probabilities that 0, 1, 2, 3, or 4 neutrons will be emitted per fragment. The yields of some of the shielded isotopes, for example Cs^{136}, have been determined radiochemically (*37*). However, the detection of a shielded nuclide in the presence of isotopic activities of much greater yield is possible only when its radiation characteristics and half-life are sufficiently different from those of the higher yield isotopes to permit identification by decay and absorption measurements. The measurement of the yield of an isotope like Xe^{130} by means of a high-sensit vity mass spectrometer avoids these difficulties and makes possible a direct and accurate determination of the independent yields of such shielded isotopes.

2. Mass Spectrometric Determination of Shielded Nuclide Yields

Kennett and Thode (*62*) examined rare gas fission products with a conventional 90° direction-focusing mass spectrometer using an electron multiplier for a detector. The sensitivity of this instrument was several orders of magnitude greater than that of an ordinary single-ion collection spectrometer and was sufficient to permit a complete analysis of the xenon isotopes including the very low yield shielded nuclides Xe^{128} and Xe^{130}, in samples containing as little as 10^{10} atoms of these isotopes. Figure 1 shows a typical mass spectrogram obtained for a sample of fission product xenon extracted from irradiated plutonium. These spectrograms showed, for the first time, the presence of Xe^{128} and Xe^{130} as fission products. Whereas the

more abundant isotopes Xe^{131}, Xe^{132}, Xe^{134}, and Xe^{136} represent the cumulative yields of their respective mass chains, the yields of Xe^{128} and Xe^{130} represent the independent yields of the shielded isotopes I^{128} and I^{130}, respectively, along with a small contribution of the independent yields of the two xenon isotopes themselves (10^{-3} of peak heights).

The determined Xe^{128}/Xe^{131} and Xe^{130}/Xe^{131} ratios are used to calculate the fraction of the 128 and 130 mass chains appearing as primary fission fragments. Consideration of the neutron capture contribution must also be made since the reactions I^{127} (n,γ) I^{128} and I^{129} (n,γ) I^{130} are both possible. From these considerations, the following relation may be derived:

(measured yield of Xe^{130}) = (independent yield of I^{130})
+ (contribution from capture in the 129 chain)

$$Y^{130} = \frac{Xe^{130}Y^{131}}{Xe^{131}} = \alpha Y^{130} + \left[1 - \frac{1 - e^{-\sigma\phi t}}{\sigma\phi t}\right] Y^{129}; \qquad (27)$$

where α is the fraction of the 130 chain formed as I^{130}; ϕ is the flux; t the irradiation time; σ the neutron capture cross section of I^{129}; and Y^A represents the total chain yield for mass number A. Actually, the neutron capture process is small at moderate neutron fluxes and in such cases the second term in Eq. (27) can be neglected. An analogous calculation gives the independent yield of I^{128}.

A similar investigation, in the krypton region revealed the presence of Kr^{80} and Kr^{82} indicating that Br^{80} and Br^{82} are also products of fission. Since the two selenium nuclides preceding the Br^{80} and Br^{82} in their respective mass chains are stable, these isotopes can only be formed directly in fission and their yields are independent yields. The independent yields of Br^{80} and Br^{82} are, therefore, determined from the yields of their daughters Kr^{80} and Kr^{82} measured mass spectrometrically. As in the analogous xenon case, the independent yields of the Kr^{80} and Kr^{82} will be less than 1% of that of the corresponding isotopes of bromine, and the total yields of these isotopes may therefore be ascribed to the parent isotopes Br^{80} and Br^{82}.

It is therefore possible, by means of a simple mass spectrometric analysis of a single fission gas sample, to determine directly and with considerable accuracy the independent yields of 4 shielded nuclides. To date, the primary yields of I^{128} and I^{130} have been determined for the thermal neutron induced fission of U^{233}, U^{235}, and Pu^{239}, and preliminary yields of Br^{80} and Br^{82} have been obtained for the thermal neutron fission of U^{233} and U^{235} (*62*).

3. Charge Distribution Postulates

The accurate independent yields of I^{128} and I^{130} obtained for U^{233}, U^{235}, and Pu^{239} fission provide a severe test for any hypothesis of charge distribu-

tion. Since both isotopes are formed as the same element and therefore the value of Z is constant, and since the most probable charge Z_p for mass chains 128 and 130 is in the region of the 50-proton shell, a discrepancy between theory and experiment might be expected here.

a. Equal chain length postulate. The early independent yield data obtained by Glendenin, Coryell, and Edwards (*38*), Glendenin (*37*), and Pappas (*88*) were sufficient to determine a semiempirical charge distribution which is assumed independent of the mass chain, the fissioning nucleus,

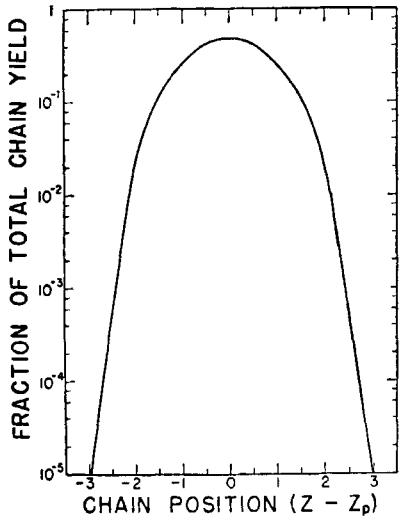

FIG. 10. The empirical charge-distribution curve as determined by Glendenin (*37*).

and the neutron energy. The hypothesis of equal charge displacement of Glendenin assumes that the most probable charges for both fragments in fission are equally displaced from the center of the valley of beta stability. The probability curve is of the Gaussian type centered around Z_p, the most probable charge for the mass chain considered, and is shown in Fig. 10. The value of Z_p is given by:

$$Z_p = Z_A - \tfrac{1}{2}[Z_A + Z_{(A^1-A-\nu+1)}] - Z^1; \tag{28}$$

where Z_A is the most stable charge for mass A which is found from the Bohr-Wheeler stability line; A^1 and Z^1 are the mass number and charge of the fissioning nucleus, and ν is the average number of neutrons emitted per fission. Therefore, the most stable charge for each fragment satisfies the equation:

$$(Z_p - Z_A)_{\text{light}} = (Z_p - Z_A)_{\text{heavy}}. \tag{29}$$

Pappas found better agreement with experimental values when he calculated the Z_p-values using the lines of maximum stability given by Coryell, Brightsen, and Pappas (*23*). These lines have discontinuities at nuclear shell boundaries. He defined Z_p by:

$$Z_p = Z_A - \tfrac{1}{2}[Z_A - Z_{(A1-A+1)} - Z^1], \tag{30}$$

so that Z_p corresponds to the mass chain $A - 1$ since prompt neutron emission is thought to occur from the fragments themselves. In most cases Z_p is nonintegral.

The most probable charge Z_p for the mass chains 128 and 130 for the various fissioning nuclei may be calculated using either the Glendenin or Pappas equation.

Figure 11 shows the determined fractional chain yields relative to the smooth curves obtained semiempirically by Glendenin and Pappas. It is

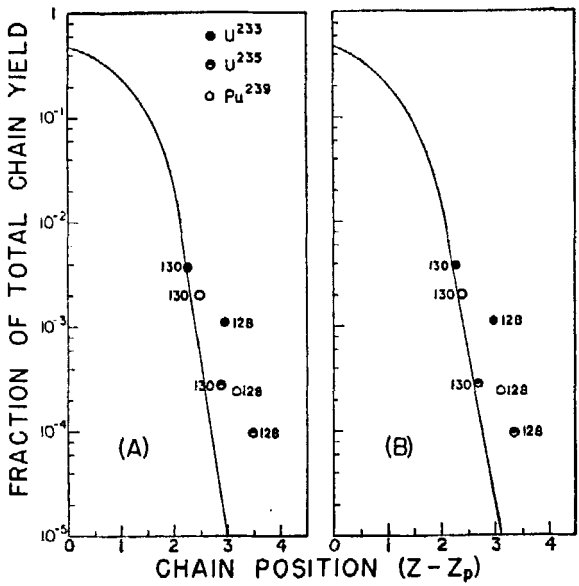

FIG. 11. Comparison of the independent yield data of I^{128} and I^{130} (*62*) with the charge-distribution curve of (A) Glendenin (*37*) and (B) Pappas (*88*).

clear that the yields do not agree with these curves and that a smooth curve cannot be drawn through all the points. In both cases, the calculated Z is too large and there is a displacement according to mass.

b. Postulate of maximum energy release. Since all the I^{130} yields lie on the curve, the assumption made by Glendenin (*37*) that the curve shown in Fig. 10 is independent of the mass and charge of the fissioning nuclide appears valid within the accuracy of the yield measurements. Also, the

assumption that the charge-distribution curve is independent of the mass of the fission fragments seems to be confirmed by radiochemical determinations. Kennett and Thode (*62*), therefore, concluded that the displacement of the I^{128} yields is due mainly to the method used to calculate Z_p. Since it might be expected that Z_p would remain close to 50 over several masses in the neighborhood of the 50-proton shell, they proposed that shell effects be taken into account more directly in the determination of Z_p for a given mass. This was done by postulating a Z_p which would yield the greatest energy release in the fission act. For example, in the fission of Pu^{239}, the value of Z_p is defined in such a way that

$$E = M(240, 94) - 3M(1,0) - M(A, Z_p) - M(237 - A, 94 - Z_p) \quad (31)$$

is maximum.

For Eq. (31) to have its maximum value, accurate values for masses far removed from the stability line are required and it is necessary to make extrapolations by means of a mass formula which will include shell effects. The mass formula of Kumar and Preston (*67*) in which shell effects and spin terms have been included, was chosen as the most applicable for the evaluation of Eq. (31). Preliminary calculations of Z_p made over the mass range $A = 126$ to $A = 136$ for U^{233}, U^{235}, and Pu^{239}, are plotted in Fig. 12. The effect of the 50-proton shell and 82-neutron shell are clearly indicated. It is seen that the value of Z_p remains very nearly 50 from $A = 128$ to $A = 132$ which is quite different from the behavior of Z_p determined from the equal chain length hypothesis shown as Z'_p in Fig. 12. It turns out that the value of Z_p calculated from energetic considerations is 0.4 charge units higher at mass 128 than that calculated from the equal chain length equation. This indicates that the charge-distribution curve is displaced by 0.4 charge units at mass 128 due to the influence of the 50-proton shell. Actually, it is seen from Fig. 11 that the measured 128 yields are displaced by 0.5 charge units in the same direction. Therefore, the independent yield results at I^{128} and I^{130} seem to support the postulate of maximum energy release for the division of nuclear charge in fission. Also, the values of Z_p calculated by the method of maximum energy release predict that the independent yields of I^{131} and I^{132} will be low and will lie to the left of the curve in Fig. 11 just as the I^{128} yields are high and lie to the right. This has been confirmed by the results of Wahl who found that the independent yields of Te^{131} and I^{132} were low. In general, independent yields plotted on the basis of a Z_p calculated from the maximum energy release postulate give a charge-distribution curve which although different from that obtained from the equal chain length postulate does account for the present independent yield data equally as well. In addition, the maximum energy release postulate does indicate shell effects when the Kumar and Preston mass formula

is used and can account for the accurately determined yields of I^{128} and I^{130} which otherwise present an anomaly.

In the evaluation of Z_p from the postulate of maximum energy release, other mass formulas may be used for extrapolating to masses far removed from the stability line. In this connection, the mass formulas of Hay and

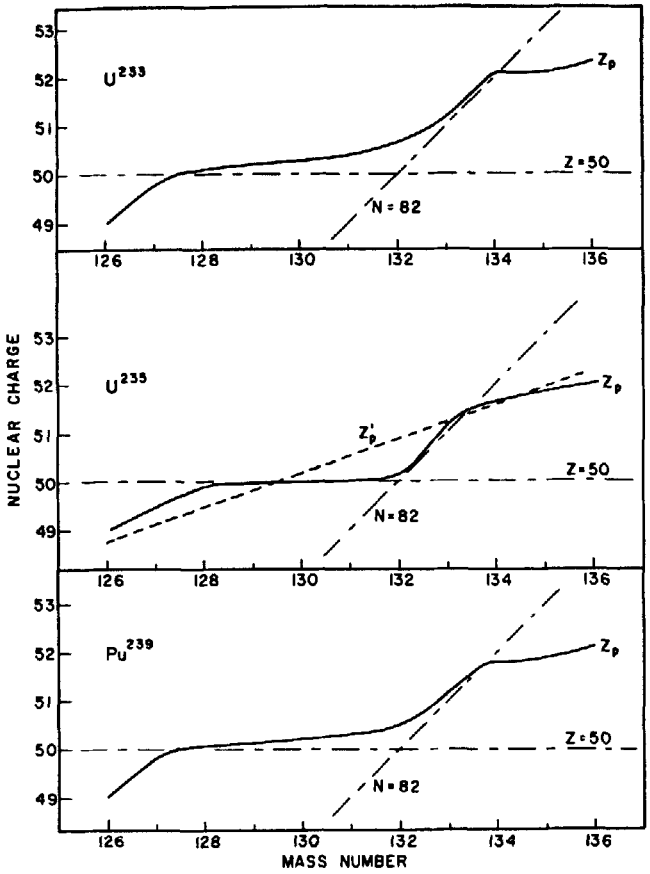

FIG. 12. Curves showing the relation between Z_p and A for the postulate of maximum energy release (*62*). Z'_p predicted by Glendenin (*37*).

Newton (*42*) and of Cameron (*17*) have been tried and the values of Z_p calculated do not show sharp discontinuities at shell crossings. The mass formula of Cameron takes shell effects and spin terms into account much as does the mass formula of Kumar and Preston, however, the mass formula of the latter is specifically used for isobaric sequences which show discontinuities in β-decay energies versus charge curves when shells are crossed.

c. Multineutron evaporation from primary fission fragments. Recently, Cameron (*18*) used the statistical theory of fission with a new mass formula as the basis for a semiempirical procedure for correlating fission yields and kinetic-energy distributions. This procedure enabled him to calculate primary yields of individual nuclides. Since his calculations indicate extremely small primary yields for nuclides near the valley of beta stability, he concluded that the small independent yields found experimentally for shielded nuclides have resulted from the evaporation of 3 or 4 neutrons from nuclei of approximately maximum primary yield on a mass chain.

He is, therefore, suggesting that in Eq. 26 for the independent yield of I^{130}, the fourth and fifth terms are dominant; whereas, in the case of other nuclides in the 130 mass chain of moderate yield, the second and third terms are dominant since single and double neutron emissions are more probable. It is clear that $Z - Z_p$, the displacement from the most probable charge, decreases from I^{131} to I^{135} and the primary yields therefore increase markedly. On the other hand, the probability of multineutron evaporation from the primary fragments will decrease as the number of neutrons emitted per fragment increases beyond one. The question arises as to the relative importance of these two effects.

If multineutron evaporation is responsible for the independent yields of shielded nuclides, then, of course, these yields would not be predicted by any simple hypothesis for the division of charge in fission which does not take into account the distribution of fission neutron numbers.

Leachman (*69*) and, more recently, Terrell (*103*) have made calculations of the probability P of emission of any given integral number of prompt neutrons from fission making certain assumptions as to the distribution of excitation energy among the fission fragments. Although the calculations are very complex and accurate experimental data are required to fix the many parameters of the theory, some estimate can be made of the probability that a fission fragment will emit a given number of neutrons. In the most favorable case for multineutron emission, where it is assumed that all the excitation energy is always on one fragment, the probabilities of 3 and 4 neutron emission are such that terms 4 and 5 of Eq. (26) could much more than account for the experimentally determined independent yield of I^{130} providing the primary yields of I^{133} and I^{134} predicted by the simple charge-distribution theories are correct. However, the primary yields predicted for I^{131} and I^{132} are too low to account for the independent yield found for I^{128} on the same basis.

The question of whether the independent yields of shielded nuclides result from multineutron evaporation from primary fragments as has been suggested is therefore still unsettled. It is perhaps significant that the independent yields of I^{128} and I^{130} for the neutron-induced fission of Pu^{239}

did not change with an increase in the neutron energy from the thermal range to the range of energies in the fission spectrum.

In any case, accurate independent yields of shielded nuclides can be determined mass spectrometrically. Interpretation of these yields will require further measurements, and, in particular, a study of the independent yields of shielded nuclides as a function of neutron energy should be of interest. In this connection, mass spectrometric methods will undoubtedly be used to determine independent yields both of shielded nuclides and short-lived isotopes for which satisfactory sweep experiments can be designed.

References

1. Aagard, P., Anderson, G., Burgman, J. O., and Pappas, A. C., *J. Inorg. & Nuclear Chem.* **5,** 105 (1957).
2. Aldrich, L. T., Wetherill, G. W., Tilton, G. R., and Davis, G. L., *Phys. Rev.* **103,** 1045 (1956).
3. Allen, J. S., *Phys. Rev.* **55,** 966 (1939).
4. Anikina, M. P., Aron, P. M., Gorshkov, V. K., Ivanov, R. N., Krizhansky, L. M., Kukavadze, G. M., Murin, A. N., Reformatsky, I. A., and Ershler, B. V., *Proc. 2nd Intern. Conf. on Peaceful Uses of Atomic Energy, Geneva* **15,** 446 (1958).
5. Ashizawa, F. T., and Kuroda, P. K., *J. Inorg. & Nuclear Chem.* **5,** 12 (1957).
6. Aston, F. W., *Phil. Mag.* [6] **38,** 707 (1919).
7. Aston, F. W., *Proc. Roy. Soc.* **A132,** 487 (1931).
8. Barnard, G. P., "Modern Mass Spectrometry." Institute of Physics, London, 1953.
9. Bartholomew, R. M., Boyd, A. W., Brown, F., Hawkins, R. C., Lounsbury, M., and Merritt, W. F., *Can. J. Phys.* **33,** 43 (1955).
10. Bay, Z., *Nature* **141,** 284, 1011 (1938); *Rev. Sci. Instr.* **12,** 127 (1941).
11. Bergstrom, I. M., *Siegbahn Commem. Volume* p. 355 (1951).
12. Bidinosti, D. R., Fickel, H. R., and Tomlinson, R. H., *Proc. 2nd Intern. Conf. on Peaceful Uses of Atomic Energy, Geneva* **15,** 459 (1958).
13. Blades, A. T., and Thode, H. G., *Z. Naturforsch.* **10a,** 838 (1955).
14. Blades, A. T., Fleming, W. H., and Thode, H. G., *Can. J. Chem.* **34,** 233 (1956).
15. Bohr, A., *Proc. 1st Intern. Conf. on Peaceful Uses of Atomic Energy, Geneva* **2,** 151 (1955).
16. Brown, F., Hall, G. R., and Walter, A. J., *J. Inorg. & Nuclear Chem.* **1,** 241 (1955).
17. Cameron, A. G. W., *Can. J. Phys.* **35,** 1021 (1957).
18. Cameron, A. G. W., *Proc. 2nd. Intern. Conf. on Peaceful Uses of Atomic Energy, Geneva* **15,** 425 (1958).
19. Campbell, N. R., and Wood, A., *Proc. Cambridge Phil. Soc.* **14,** 15 (1907).
20. Classen, J., *Jahrb. Hamburg. Wiss. Anst. Beiheft* (1907).
21. Cohen, A. A., *Phys. Rev.* **63,** 219 (1943).
22. Cork, J. M., Shriffer, R. G., and Fowler, C. M., *Phys. Rev.* **74,** 1657 (1948).
23. Coryell, C. D., Brightsen, R., and Pappas, A. C., *Phys. Rev.* **85,** 732 (1952).
24. Dempster, A. J., *Phys. Rev.* **11,** 316 (1918).
25. Dempster, A. J., *Phys. Rev.* **71,** 829 (1947).
26. Duckworth, H. E., "Mass Spectroscopy." Cambridge University Press, London and New York, 1958.

27. Fickel, H. R., and Tomlinson, R. H., unpublished work, McMaster University, Hamilton, Canada (1958).
28. Fickel, H. R., and Tomlinson, R. H., *Can. J. Phys.* **37,** 531 (1959).
29. Fickel, H. R., and Tomlinson, R. H., *Can. J. Phys.* **37,** 916, 926 (1959).
30. Fleming, W. H., and Thode, H. G., *Phys. Rev.* **92,** 378 (1953).
31. Fleming, W. H., Tomlinson, R. H., and Thode, H. G., *Can. J. Phys.* **32,** 522 (1954).
32. Fleming, W. H., and Thode, H. G., *Can. J. Chem.* **34,** 193 (1956).
33. Fong, P., *Phys. Rev.* **89,** 434 (1953).
34. Frenkel, J., *J. Phys. (U.S.S.R.)* **10,** 533 (1946).
35. Fritze, K., McMullen, C. C., and Thode, H. G., *Proc. 2nd Intern. Conf. on Peaceful Uses of Atomic Energy, Geneva* **15,** 436 (1958).
36. Fritze, K., McMullen, C. C., and Thode, H. G., unpublished work, McMaster University, Hamilton, Canada (1958).
37. Glendenin, L. E., Tech. Rept. No. 35, Laboratory for Nuclear Sci. and Eng., M. I. T. (1953); also Ph.D. thesis M. I. T. (1949).
38. Glendenin, L. E., Coryell, C. D., and Edwards, R. R., in "National Nuclear Energy Series," Div. IV. Vol. 9, p. 489. Paper 52. McGraw-Hill, New York, 1951.
39. Glendenin, L. E., Steinberg, E. P., Inghram, M. G., and Hess, D. C., *Phys. Rev.* **84,** 860 (1951).
40. Glendenin, L. E., Steinberg, E. P., Flynn, K. F., Hayden, R. J., and Inghram, M. G., Mass spectrometric data quoted by E. P. Steinberg and L. E. Glendenin, *Proc. 1st Intern Conf. on Peaceful Uses of Atomic Energy, Geneva* **7,** 3 (1955).
41. Grandsen, M. M., and Boyle, W. S., *Phys. Rev.* **82,** 447 (1951).
42. Hay, I. W., and Newton, T. D., *Can. J. Phys.* **35,** 195 (1957).
43. Hayden, R. J., *Phys. Rev.* **74,** 650 (1948).
44. Hayden, R. J., Reynolds, J. H., and Inghram, M. G., *Phys. Rev.* **75,** 1500 (1949).
45. Hertzberg, G., "Spectra of Diatomic Molecules." Van Nostrand, New York, 1950.
46. Hemmendinger, A., and Smythe, W. R., *Phys. Rev.* **51,** 1052 (1937).
47. Hess, D. C., Hayden, R. J., and Inghram, M. G., *Phys. Rev.* **72,** 730 (1947).
48. Hess, D. C., and Inghram, M. G., *Phys. Rev.* **76,** 300 (1949).
49. Hevesy, G., and Paneth, F. A., "A Manual of Radioactivity," 2nd ed. Oxford University Press, London and New York, 1938.
50. Hill, D. J., and Wheeler, J. A., *Phys. Rev.* **89,** 1102 (1953).
51. Hill, D. J., *Proc. 2nd Intern. Conf. on Peaceful Uses of Atomic Energy, Geneva* **15,** 244 (1958).
52. Hill, R. D., *Phys. Rev.* **98,** 1272 (1955).
53. Hoagland, E. J., and Sugarman, N., *in* "National Nuclear Energy Series," Div. IV, Vol. 9, p. 635. Paper 69. McGraw-Hill, New York, 1951.
54. Inghram, M. G., Hess, D. C., and Hayden, R. J., *Phys. Rev.* **71,** 561 (1947).
55. Inghram, M. G., Hayden, R. J., and Hess, D. C., *Phys. Rev.* **79,** 271 (1950).
56. Inghram, M. G., and Chupka, W. A., *Rev. Sci. Instr.* **24,** 518 (1953).
57. Inghram, M. G., *J. Phys. Chem.* **57,**809 (1953).
58. Inghram, M. G., and Hayden, R. J., "A Handbook of Mass Spectroscopy," Nuclear Sci. Series, Report No. 14. National Academy of Sciences, National Research Council, Washington, D. C., 1954.
59. Inghram, M. G., *Ann. Rev. Nuclear Sci.* **4,** 81 (1954).
60. Katcoff, S., and Rubinson, W., *Phys. Rev.* **91,** 1458 (1953).
61. Katcoff, S., *Nucleonics* **16,** No. 4, 78 (1958).
62. Kennett, T. J., and Thode, H. G., *Phys. Rev.* **103,** 323 (1956).

63. Kennett, T. J., and Thode, H. G., *J. Inorg. & Nuclear Chem.* **5,** 253 (1958).
64. Kennett, T. J., and Thode, H. G., *Can. J. Phys.* **35,** 969 (1957).
65. Kienberger, C. A., *Phys. Rev.* **76,** 1561 (1949).
66. Krizhansky, L. M., Maly, Ya., Murin, A. N., and Preobrazhensky, B. K. *Soviet J. Atomic Energy* **2,** 334 (1957).
67. Kumar, K., and Preston, M. A., *Can. J. Phys.* **33,** 298 (1955).
68. Lapp, R. E., Van Horn, J. R., and Dempster, A. J., *Phys. Rev.* **71,** 745 (1947).
69. Leachman, R. B., *Phys. Rev.* **101,** 1005 (1956).
70. Leachman, R. B., *Proc. 2nd Intern. Conf. on Peaceful Uses of Atomic Energy, Geneva* **15,** 229 (1958).
71. Lewis, L. G., and Hayden, R. J., *Rev. Sci. Instr.* **19,** 599 (1948).
72. Lewis, L. G., and Hayden, R. J., *Rev. Sci. Instr.* **19,** 922 (1948).
73. Lindner, M., *Phys. Rev.* **84,** 240 (1951).
74. Macnamara, J., Collins, C. B., and Thode, H. G., *Phys. Rev.* **75,** 532 (1949).
75. Macnamara, J., and Thode, H. G., *Phys. Rev.* **80,** 471 (1950).
76. Macnamara, J., and Thode, H. G., *Phys. Rev.* **80,** 296 (1950).
77. Macnamara, J., Collins, C. B., and Thode, H. G., *Phys. Rev.* **78,** 129 (1950)
78. Mattauch, J., *Naturwissenschaften* **25,** 189 (1937).
79. Mayer, M. G., *Phys. Rev.* **74,** 235 (1948).
80. McMillan, E. M., *Phys. Rev.* **72,** 591 (1947).
81. Meitner, L., *Arkiv Fysik* **4,** 383 (1951).
82. Melaika, E. A., Parker, M. J., Petruska, J. A., and Tomlinson, R. H., *Can. J. Chem.* **33,** 830 (1955).
83. Michel, M. C., and Templeton, D. H., *Phys. Rev.* **93,** 1422 (1954).
84. Newton, T. D., *Atomic Energy Can. Ltd., Chalk River Rept.* **C-642-A,** p. 307 (1956).
85. Nier, A. O., *Rev. Sci. Instr.* **6,** 254 (1935).
86. Nier, A. O., *Phys. Rev.* **77,** 789 (1950); **79,** 450 (1950).
87. Pappas, A. C., *Proc. 1st Intern. Conf. on Peaceful Uses of Atomic Energy, Geneva* **7,** 19 (1955).
88. Pappas, A. C., Tech. Rept. No. 63, Laboratory for Nuclear Sci. M. I. T. (1953).
89. Parker, P. L., and Kuroda, P. K., *J. Inorg. & Nuclear Chem.* **5,** 153 (1958).
90. Petruska, J. A., Thode, H. G., and Tomlinson, R. H., *Can. J. Phys.* **33,** 693 (1955).
91. Petruska, J. A., Melaika, E. A., and Tomlinson, R. H., *Can. J. Phys.* **33,** 640 (1955).
92. Petrzhak, K. A., and Flerov, G. N., *J. Exptl. Theoret. Phys. U.S.S.R.* **10,** 1013 (1949).
93. Rall, W., *Phys. Rev.* **70,** 112 (1946).
94. Rittenberg, D., *J. Appl. Phys.* **13,** 561 (1942).
95. Segre, E., *Phys. Rev.* **86,** 21 (1952).
96. Sellers, P. A., Stevens, C. M., and Studier, M. H., *Phys. Rev.* **94,** 952 (1954).
97. Smythe, W. R., and Hemmendinger, A., *Phys. Rev.* **51,** 178 (1937).
98. Snell, A. H., *Phys. Rev.* **52,** 1007 (1937).
99. Snell, A. H., Levinger, J. S., Meiners, E. P., Sampson, M. B., and Wilkinson, R., *Phys. Rev.* **72,** 545 (1947).
100. Steinberg, E. P., Glendenin, L. E., Inghram, M. G., and Hayden, R. J., *Phys. Rev.* **95,** 867 (1954).
101. Strassmann, F., and Walling, E., *Ber. deut. chem. Ges.* **71B,** 1 (1938).
102. Swiatecki, W. J., *Phys. Rev.* **83,** 178 (1951).
103. Terrell, J., *Phys. Rev.* **108,** 783 (1957).
104. Thode, H. G., and Graham, R. L., *Can. J. Research* **A25,** 1 (1947); Montreal Report MX 129 Natl. Research Council of Canada (1945).

105. Thode, H. G., *Nucleonics* **3,** 14 (1948).
106. Thode, H. G., *Ann. Rev. Phys. Chem.* **4,** 95 (1953).
107. Thomson, J. J., *Proc. Roy. Soc.* **A89,** 1 (1914).
108. Vladimirsky, J., *J. Exptl. Theoret. Phys. U.S.S.R.* **32,** 822 (1957).
109. Wahl, A. C., *J. Inorg. & Nuclear Chem.* **6,** 263 (1958).
110. Walker, W. H., Ph.D. thesis, McMaster University, Hamilton, Canada (1954).
111. Walker, W. H., and Thode, H. G., *Phys. Rev.* **90,** 447 (1953).
112. Wanless, R. K., and Thode, H. G., *Can. J. Phys.* **31,** 517 (1953).
113. Wanless, R. K., and Thode, H. G., *Can. J. Phys.* **33,** 541 (1955).
114. Weinberg, A. M., and Wigner, E. P., "Physical Theory of Neutron Chain Reactors," p. 106. University of Chicago Press, Chicago, Ill., 1958.
115. Westcott, C. H., Walker, W. H., and Alexander, T. K., *Proc. 2nd Intern. Conf. on Peaceful Uses of Atomic Energy, Geneva* **16,** 202 (1958).
116. Westcott, C. H., Chalk River Publ. No. 407, Atomic Energy of Canada Ltd. (1957).
117. Wetherill, G. W., *Phys. Rev.* **92,** 907 (1953).
118. White, F. A., and Collins, T. L., *Appl. Spectroscopy* **8,** No. 4, 169 (1954).
119. White, F. A., Collins, T. L., and Rourke, F. M., *Phys. Rev.* **97,** 566 (1955).
120. White, F. A., Collins, T. L., and Rourke, F. M., *Phys. Rev.* **101,** 1786 (1956).
121. Wiles, D. R., Smith, B. W., Horsley, R., and Thode, H. G., *Can. J. Phys.* **31,** 419 (1953).
122. Wiles, D. M., and Tomlinson, R. H., *Phys. Rev.* **99,** 188 (1955).
123. Wiles, D. M., and Tomlinson, R. H., *Can. J. Phys.* **33,** 133 (1955).
124. Wiles, D. M., Petruska, J. A., and Tomlinson, R. H., *Can. J. Chem.* **34,** 227 (1956).
125. Wilson, R. R., *Phys. Rev.* **72,** 189 (1947).
126. Young, B. G., and Thode, H. G., *Can. J. Phys.* **38,** 1 (1960).